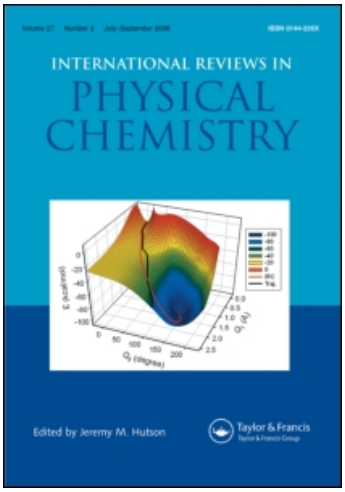

International Reviews in Physical Chemistry
Publication details, including instructions for authors and subscription information:
http://www.informaworld.com/smpp/title~content=t713724383

Structure, spectroscopy and dynamics of halogen molecules interacting with water

Margarita I. Bernal-Uruchurtu[a]; Galina Kerenskaya[a]; Kenneth C. Janda[a]
[a] Department of Chemistry, University of California, Irvine, California, USA

To cite this Article Bernal-Uruchurtu, Margarita I. , Kerenskaya, Galina and Janda, Kenneth C.(2009) 'Structure, spectroscopy and dynamics of halogen molecules interacting with water', International Reviews in Physical Chemistry, 28: 2, 223 — 265
To link to this Article: DOI: 10.1080/01442350903017302
URL: http://dx.doi.org/10.1080/01442350903017302

International Reviews in Physical Chemistry
Vol. 28, No. 2, April–June 2009, 223–265

Taylor & Francis
Taylor & Francis Group

Structure, spectroscopy and dynamics of halogen molecules interacting with water

Margarita I. Bernal-Uruchurtu[§], Galina Kerenskaya and Kenneth C. Janda*

Department of Chemistry, University of California, Irvine, California, USA

(*Received 24 March 2009; final version received 29 April 2009*)

Immediately on the discovery of the halogen molecules, their chemistry was closely linked with that of water. For some time, it was thought that water was a constituent of chlorine. The brightly coloured halogens have played an important role in spectroscopy almost from the beginning of its use as a quantitative tool for understanding molecular structure. Already in the 19th century, the remarkable colour change upon dissolving iodine in aqueous solution was noted and studied. However, a complete, microscopic explanation for this phenomenon is yet to be achieved. We review this field and propose that the time is right to achieve this fundamental goal of chemical physics for the halogen–water system. In addition, we review recent work on the UV-vis, Raman and ultrafast dynamics studies of halogen molecules in clathrate hydrate cages, spectroscopy of water–halogen dimer molecules and theory of small water–halogen clusters. Based on recent findings, we propose a variety of 'next steps' for the complete understanding of this fascinating model system.

Keywords: halogen bonding; halogen hydrate; bromine hydrate; aqueous solution; UV-vis spectroscopy; Raman spectroscopy; water–halogen dimers; *ab initio* theory; simulated spectra

Contents

*Corresponding author. Email: kcjanda@uci.edu
[§]On leave from Centro de Investigaciones Químicas, Universidad Autónoma del Estado de Morelos, México; mabel@uaem.mx.

ISSN 0144–235X print/ISSN 1366–591X online

DOI: 10.1080/01442350903017302
http://www.informaworld.com

1. Introduction

An often-stated goal of chemical physics is to understand the properties of macroscopic systems based on a complete account of the microscopic interactions. The halogen–water system is a very interesting case study for moving towards this goal. Halogen molecules are unusual diatomic molecules in that they have rich valence electronic spectra that extend into the visible region and yet they are relatively stable. As such, halogen molecules are often used for studying intermolecular forces in clusters and condensed phase systems and this leads to model studies for *ab initio* calculations. As for hydrogen bonding, the intermolecular forces between electron donor molecules and halogen molecules are strong enough to be considered as a special class. These strong intermolecular forces have proved to be a fascinating complication almost from the discovery of the halogens. Two hundred years ago, while trying to measure the melting temperature of chlorine, Humphrey Davy discovered what later proved to be chlorine hydrate [1]. Although there is no formal bonding between the water and the chlorine, the melting point of this substance is 10°C. One hundred and forty years later, Pauling and Marsh determined the structure of the hydrate by X-ray crystallography [2]. Another 46 years elapsed before the structure of bromine hydrate was determined [3].

Another fascinating property of the halogens is the remarkable solvent shifts of their electronic spectra. In aqueous solution the valence absorption spectrum of iodine is blue shifted by 3000 cm^{-1} [4,5]. A dilute solution of iodine in hexane is a deep purple colour since green and yellow light are strongly absorbed. An aqueous solution is yellow–orange since the absorption has shifted to the middle of the blue portion of the spectrum. This strong

spectral shift has resisted a detailed interpretation in terms of specific interactions. Even in their weak interactions the halogens are unusual. In spite of the fact that the zero point energy of the ground vibrational levels of He–Br_2 and He–I_2 are above all the barriers to internal rotation, two distinct isomers have been observed: one linear, one 'T' shaped [6–8]. In this review we seek to summarise these and other equally interesting results, explain the current level of interpretation and suggest useful next steps toward a complete microscopic understanding of the interaction between halogen molecules and water.

This review will concentrate on the interaction of Cl_2, Br_2 and I_2 with water. F_2 is not stable in aqueous solution and its valence excitation transitions are very weak. Similarly, there is not much data available on the interaction of the interhalogens with water, except for several of the dimers. Aqueous solutions of the interhalogens tend to be extremely complicated due to disproportionation and other reactions. A particularly interesting case is BrCl. When either BrCl or a mixture of Br_2 and Cl_2 is brought into contact with water at 10°C, crystals are formed that are stable at temperatures well above the dissociation temperatures of either chlorine hydrate or bromine hydrate [9]. To our knowledge the ratio of Cl_2, Br_2 and BrCl in these crystals is yet to be determined except that they appear to be rich in bromine.

1.1. *Halogens in clathrate hydrates*

As any chemistry student should know, the halogen molecules are quite reactive and therefore dangerous if handled improperly. This is reflected in their early history. Chlorine was the first of the halogens to be isolated. Although Scheele prepared a sample in 1774, he did not immediately recognise it as an element. Since it was thought to be a part of a mixture that contained oxygen, in 1809 Guy Lussac and Thénard [10] tried to remove the oxygen by reacting it with charcoal. When this experiment failed they considered the possibility that it might be an element. In 1811, Sir Humphrey Davy [1] repeated the experiment, declared it to be an element and named it chlorine. While cooling the gas over an aqueous solution, Davy unknowingly produced the first synthetic clathrate hydrate solid at 10°C. Even now, most chemists are surprised the first time they learn that a mixture of chlorine and water has a 'melting point' higher than that of water itself since most textbooks declare that impurities lower the melting points of liquids. An interesting misconception is embodied in the title of an 1818 publication of Davy [11]: 'On the fallacy of the experiments in which water is said to have been formed by the decomposition of chlorine'. It wasn't until 1823, that Faraday [12] was able to liquefy chlorine for the first time.

In 1823, Faraday [13] found the composition of chlorine hydrate to be about 10 : 1 $H_2O : Cl_2$. The details of how the clathrate hydrates could have a variable stoichiometry started to be unravelled in the 1940s when von Stackelberg and his collaborators [14] first applied X-ray methods to their crystals. They found that some guest molecules induced the formation of a lattice with a 17 Å unit cell, and that others, including Cl_2, induced the formation of crystals with a 12 Å unit cell. Claussen-deduced structures [15,16], now known as CS-I (12 Å unit cell) and CS-II (17 Å unit cell) consistent with each of these unit cell dimensions. Soon after, Pauling and Marsh [2] recorded new data for chlorine hydrate and showed that it is consistent with what is now called the CS-I structure.

The essence of the clathrate hydrate structures can be visualised by considering combinations of the polyhedra illustrated in Figure 1. If 20 water molecules combine to form

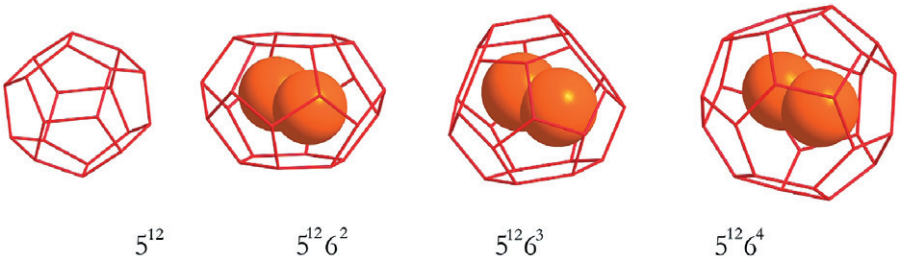

Figure 1. [Colour online] This figure illustrates four hydrate cage types that are important to this review. Each cage vertex is an oxygen atom and each edge contains a hydrogen atom. Each vertex is also connected to a neighbouring cage via a hydrogen bond. The naming formula gives the number of pentagonal and hexagonal faces. The 5^{12} and $5^{12}6^4$ cages are nearly spherical with diameters of 8.1 and 9.6 Å, respectively. The $5^{12}6^2$ cage is oblate with diameter = 8.7 Å and height = 8.3 Å. The $5^{12}6^3$ cage is prolate with diameter = 9.1 Å and length = 10.0 Å. The van der Waals radius of oxygen is usually taken to be 1.5 Å for calculating the available cage dimensions for guest molecules. Reproduced, with permission, form ref. [24].

a 'dodecahedral cluster' such as illustrated in Figure 1, the centre of the cluster is an empty space that can trap a guest atom or molecule. In this case, a xenon atom is almost ideally suited to fit in the cluster so that the van der Waals and electrostatic interactions between the Xe atom (vdW diameter = 4.3 Å) [17] and the water molecules are attractive and serve to stabilise the cluster. Since this cluster has 12 pentagonal faces, it is commonly referred to as a 5^{12} cage. A slightly larger cage formed from 24 water molecules with hexagonal faces on top and bottom and 12 pentagonal faces forming the sides is referred to as a $5^{12}6^2$ cage. Such a cage has an interior volume favourable for trapping chlorine molecules ($l_{vdW} = 5.5$ Å) (The van der Waals length is estimated as the sum of the bond length plus the van der Waals radii of the atoms [17].). The next larger $5^{12}6^3$ cage formed from 26 water molecules efficiently traps bromine ($l_{vdW} = 6.0$ Å). The still larger $5^{12}6^4$ cage formed from 28 water molecules is large enough to trap an iodine molecule ($l_{vdW} = 6.62$ Å).

Just as pentagonal tiles cannot be used to tile a 2D surface, none of the hydrate cages in Figure 1 can be used alone as a building block to form a 3D crystal. The CS-II structure proposed by Clausen combined two 5^{12} cages with each $5^{12}6^4$ cage to form a unit cell with $a_o = 17$ Å that contains 136 water molecules, 16 smaller cavities and eight larger cavities. If there were one guest molecule in every cavity, the stoichiometric ratio would be H_2O: guest = 136 : 24 = 5.67. At the other limit, if the guest molecule only fits in the larger cage, the stoichiometric ratio would be H_2O : guest = 136 : 8 = 17. Since the host and guest molecule are not chemically bonded, the clathrate structure is referred to as a solid solution, and the variable stoichiometry is no longer a mystery [18]. The CS-I structure combines one 5^{12} cage for every three $5^{12}6^2$ cages to form a unit cell that contains 46 water molecules, two small cavities and six medium-sized cavities as shown in Figure 2. Pauling and Marsh achieved the best fit to their data when they assumed that chlorine molecules only fit into the $5^{12}6^2$ cages yielding a stoichiometric ratio of H_2O : guest = 46 : 6 = 7.67. Thirty years later Cady [19] performed careful stoichiometric studies at 0°C that yielded stoichiometric ratios between 7.28 for $P(Cl_2) = 0.46$ atm and 6.20 for $P(Cl_2) = 3.35$ atm. If we assume that each of the $5^{12}6^2$ cages contain a Cl_2 molecule, then between 15% and 70% of the smaller cages also contain one Cl_2 molecule. This is in conflict with the assumption of Pauling and Marsh that the 5^{12} cage is too small to contain a Cl_2 molecule if one assumes normal van der Waals radii. So, in

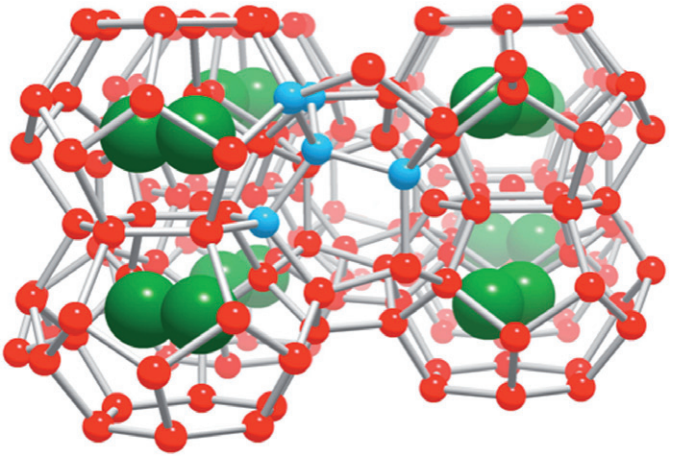

Figure 2. [Colour online] This figure shows a portion of the CS-I structure. Only the $5^{12}6^2$ cages are shown. The 5^{12} cages would fill in the gaps. The chlorine molecules are shown to illustrate the relative size. Little is known about any correlation of the chlorine molecule orientation with either the cage geometry or with adjacent chlorine molecules.

this regard, the 'radius' of the H_2O–Cl_2 interaction is smaller than expected. This will be a recurring theme in the work presented below.

Determining the structure of bromine hydrate has been especially difficult. A tetragonal unit cell was determined in 1963 by Allen and Jeffrey [20]. However, the variable stoichiometry and crystal shapes and the earlier findings of a cubic unit cell [14] persuaded many investigators that several crystalline forms could coexist [21,22]. In 1997, Udachin *et al.* [23] determined that a wide variety of bromine hydrate crystal shapes and stoichiometry all correspond to the Allen and Jeffrey tetragonal unit cell made up of 5^{12}, $5^{12}6^2$ and $5^{12}6^3$ cages in a 10:16:4 ratio. We will refer to this structure as tetragonal structure I, or TS-I. If all of the $5^{12}6^2$ and $5^{12}6^3$ cages are occupied, then the limiting unit cell stoichiometry is $(Br_2)_{20}(H_2O)_{172}$; one bromine molecule for every 8.6 water molecules. Incomplete cage filling could account for $H_2O : Br_2$ ratios as high as 10.7. Below, we will review new results from Irvine that convince us that that three different crystal structures can readily be observed for bromine hydrate: the TS-I structure determined by Udachin *et al.*, and also both of the more common hydrate structures, CS-I and CS-II. We believe the CS-I structure to be metastable for bromine, but kinetically preferred under certain formation conditions. Our evidence strongly suggests that the CS-II structure is the stable form for a range of temperatures and compositions. Thus it appears that at least three bromine hydrate crystal structures have chemical potentials that are quite similar. Which one is the stable form under specific conditions is very sensitive to the details of the H_2O–Br_2 interaction [24,25].

We have not been able to find any reports of iodine clathrate hydrate. However, our recent work shows that iodine can be trapped in $5^{12}6^4$ cages, substituting for other guest molecules [26]. We have measured both visible and Raman spectra for such trapped molecules and the results will be discussed below.

In spite of the many interesting properties of halogen clathrate hydrates, there have been few spectroscopic studies of these solids, and no UV-vis studies were performed before the studies in Irvine that stimulated this review. As will be discussed below, the

gas–solid solutions formed by halogen molecules in clathrate hydrate cages yield quite different spectra than those of aqueous solutions or clusters.

1.2. *Halogens in aqueous solutions*

Liquid aqueous solutions of halogen molecules are even more complicated than clathrate hydrate, gas–solid, solutions. A major difficulty is the tendency of halogen molecules to react with water to form ions. This is especially a problem for Cl_2, for which the reaction: $Cl_{2(aq)} = H^+ + Cl^- + HOCl$ has a $K_{eq} = 4.2 \times 10^{-4}$ [27]. At 25°C, a saturated $Cl_{2(aq)}$ solution contains 0.061 mol L^{-1} of Cl_2 and 0.030 mol L^{-1} of Cl^- and HOCl. Cl^- combines with Cl_2 to form Cl_3^-. It is also important to limit the OH^- concentration if the spectra of the aqueous halogens are to be measured since the reactions $X_2 + 2OH^- = X^- + XO^- + H_2O$ have large equilibrium constants, again, especially for Cl_2. Since the spectra of the ionic species are much more intense than those of the neutrals, it can be difficult to determine the spectrum of aqueous Cl_2. This is less of a problem for Br_2 and I_2 for which the analogous equilibrium constants in pure water are much smaller. Their solubilities are 0.21 and 0.0013 mol L^{-1}, respectively [27]. The much higher solubility of Br_2 relative to Cl_2 and, especially I_2 is another interesting phenomenon yet to be explained on the microscopic scale.

As will be discussed in more detail below, the UV-vis spectra of halogen molecules are very sensitive to the local environment. In many cases, for instance pH indicators, such

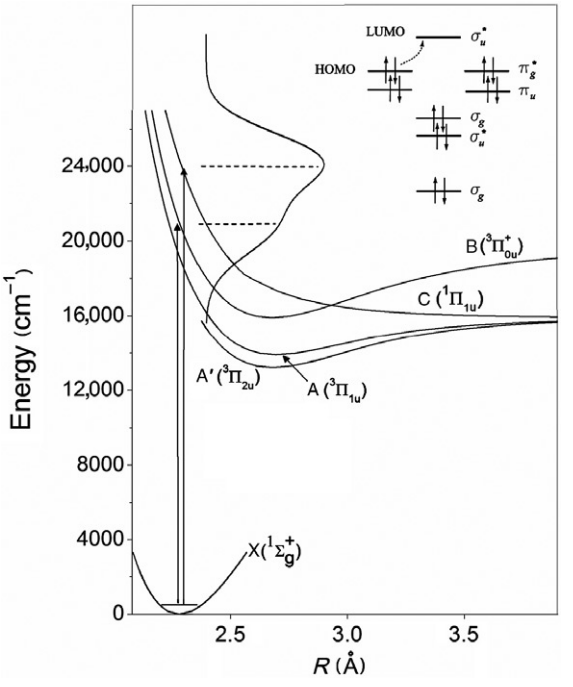

Figure 3. Ground and valence excited state potential curves of Br_2 and the two most intense electronic transitions that contribute to the UV-vis spectrum. The inset shows a molecular orbital diagram. See text for more detail. Reproduced, with permission, form ref. [24].

sensitivity is associated with structural changes. This is not the case for halogens. Before reviewing the spectroscopy of the halogens in aqueous solution, a brief review of their gas phase spectra will be useful. Figure 3 shows the UV-vis spectrum of Br_2 and offers a pictorial interpretation. For the ground state, called the **X** state, the orbitals are filled up to the π^* level; often referred to as the highest occupied molecular orbitals or HOMOs. The lowest energy electronic excitation involves the promotion of one electron from the HOMO to the σ^* lowest unoccupied molecular orbital, or LUMO. Due to spin–orbit coupling, many valence excited electronic states are associated with the transition of a single electron from the HOMO to the LUMO in the molecular orbital approximation. The three commonly observed states are referred to as the **A**, **B** and **C** states. They differ in their angular momentum symmetry.

The absorption spectroscopy of Cl_2, Br_2 and I_2 are dominated by two of these valence excited states. One, commonly called the **C** state, is repulsive so that the $\mathbf{X} \rightarrow \mathbf{C}$ absorption spectrum is smooth and continuous, even in the gas phase. The other important excited state, commonly called the **B** state, occurs to slightly lower energy of the **C** state because the **B** state has a bonding well while the **C** state is repulsive. In the gas phase the $\mathbf{X} \rightarrow \mathbf{B}$ band contains a structured portion due to bound–bound transitions and also a continuum due to transitions to energies above the dissociation limit. The **B** and **C** states are close in energy and result in overlapping spectra. In the Russell–Saunders coupling limit, the **B** state is a triplet state and the $\mathbf{X} \rightarrow \mathbf{B}$ transition is only allowed due to spin–orbit coupling. Thus, this transition is quite weak for Cl_2, and grows in intensity for Br_2 and I_2. In the spectrum for Br_2, shown in Figure 3, the $\mathbf{X} \rightarrow \mathbf{B}$ transition forms a shoulder on the low energy side of the stronger $\mathbf{X} \rightarrow \mathbf{C}$ transition. Each of the three molecules also exhibit a weak $\mathbf{X} \rightarrow \mathbf{A}$ transition to the red of the other two. Usually this band is too weak to analyse with any confidence except in the gas phase.

The peak of the bromine absorption is in the near UV range, resulting in its red colour. For Cl_2 the spectra are dominated by the stronger $\mathbf{X} \rightarrow \mathbf{C}$ transition, mostly in the UV range, resulting in the pale yellow colour of chlorine gas. For I_2 the two transitions blend together over much of the visible spectral range, resulting in the purple, almost black, colour of solid iodine.

Figure 4. Photograph of dilute solutions of I_2 in (from left to right): cyclohexane, dichloromethane and water.

Already at the end of the 19th century, it was recognised that the solvent shifts for halogen molecules were unusually large [4,5]. This is illustrated in Figure 4 for I_2 in three solvents. In cyclohexane, the I_2 spectrum is hardly shifted but is slightly broader than in the gas phase. This is referred to as an inactive solvent. In water, the valence absorption bands are shifted from $3000\,cm^{-1}$ to the blue of the gas phase and are significantly broader. Water is referred to as an active solvent. The activity of CCl_4 is between that of water and cyclohexane. In 1909, Hildebrand and Glascock [28] reported a study of adding active solvent molecules to an inactive solvent and extracting equilibrium constants for the bonding between the I_2 and the active solvent molecules.

The idea that charge transfer complexes are important in explaining halogen solvent shifts was reinforced by the study of halogens interacting with aromatic hydrocarbons [29]. However, in a 1949 Nature paper Bayliss [30] firmly stated that for bromine and iodine '*the spectra can be accounted for almost quantitatively on the basis of the physical properties of the solvents without postulating any special solvent–solute interaction*'. Mulliken was not convinced, and a year later he proposed a charge transfer complex in which the oxygen atom of ether molecules would point toward the centre of the I_2 molecule, which would be perpendicular to the C–O–C plane. Mulliken [31] suggested that the analogous structure is important for $H_2O\cdots I_2$. Without speculating on the structure, in 1954 Ham [32] confirmed that complexes are responsible for the large blue shift in the iodine–diethylether, $\sim 4000\,cm^{-1}$. After this time, we have not been able to find further work on the effect of complexation on the spectra of halogens in water or other electron donating solvents. Even for I_2 in less strongly interacting solvents like heptane and CCl_4, Gray *et al.* [33], concluded in 2001 that '*it is worth asking whether such a physical model might also work better for the solution spectra. The answer to that question must remain a topic for future study*'. Now that modern theory offers a detailed description for solvent effects on simpler systems, [34] it may be time to return to the halogens.

2. Experimental studies of H_2O–X_2

Two experimental developments provided the opportunity to study the interactions between molecules in much greater detail than is possible in aqueous solution: matrix isolation spectroscopy and the application of supersonic expansion technology to molecular beam spectroscopy. In the case of the subject for this review, each of these technologies provided the opportunity to combine a single electron donor molecule like H_2O with a single halogen molecule and obtain the spectrum of the resulting dimer. In addition to giving more detailed information for the individual clusters, these techniques allow problems associated with safety and chemical reactivity to be surmounted so that a systematic study of the halogens and interhalogens could be carried out to explore periodic trends in their properties. Matrix isolation experiments were the first tool used for infrared spectroscopy on complexes between water molecules and dihalogens since it allowed for sufficient concentrations of weakly bonded complexes to be prepared. Most of what we know regarding the geometric structures of complexes formed between halogens and donor molecules is the result of years of careful interpretation of the spectroscopic constants derived from analysis of rotational spectra generated by supersonic expansion technology.

2.1. *Matrix isolation spectroscopy*

The interest in electron donation to the halogens was stimulated by the reports on the interaction between iodine and ether molecules; first by Mulliken [31], and later by Hassel and Romming [35]. Those works led to speculation on the nature of the interactions that stabilise these types of complexes. In 1973, Fredin and Nelander [36] studied the complex formed between water and chlorine in N_2 matrices at 20 K to probe the interactions between halogen molecules and donor moieties. The vibrational frequencies of the water in the water–chlorine dimer complex were hardly changed from those of uncomplexed water, especially for the bending vibration. They concluded that the complex did not have a hydrogen bonded structure. Somewhat later, the same group recorded higher resolution spectra for water–hydrogen halide and water–halogen complexes and observed a temperature-dependent fine structure in the fundamental O–H stretching modes [37]. They concluded that the $H_2O\cdots HX$ complexes are planar while the $H_2O\cdots X_2$ complexes probably are not.

The comparison of the vibrational spectra recorded in Ar matrices clearly showed that there were significant differences between the complexes of water and the hydrogen halides and with the dihalogens. Even if the data was not conclusive, it pointed to a weaker interaction between the dihalogens and water [38]. One interesting feature of these experiments was that, in contrast with the halogen halides, for the dihalogen complexes, it was possible to observe that the intermolecular bend modes and the axial rotation of the complex were coupled. This series of detailed experiments lead to the conclusion that in all these complexes water acts as a lone pair donor.

Among the advantages of studying complexes in cold matrices is the possibility of isolating and studying pre-reactive complexes. For example, Noble and Pimentel studied the highly exothermic reaction between water and fluorine in an N_2 matrix, identified the hypofluorite molecule, HOF, and observed it interacting with another F_2 molecule [39]. Later, McInnis and Andrews [40] revisited this reaction using cold deposition in Ar matrices at 12 ± 1 K. This allowed them to isolate and characterise the $H_2O\cdots F_2$ complex. The polarisation of the halogen by water activated the F_2 stretching band. Also, the symmetric O–H stretch mode of water was enhanced, which allowed them to assign the structure as $H_2O\cdots F_2$, i.e. that oxygen acts as a lone pair donor. McInnis and Andrews [40], also studied the photochemistry of the H_2O and F_2 in Ar matrices and observed three major products, each an isomeric arrangement of HF and HOF: $FH\cdots FOH$, $FH\cdots OHF$ and $HF\cdots HOF$. $HF\cdots HOF$ is the most stable and was the only isomer detected when the experiment was performed in an N_2 matrix. That same year, Johnsson *et al.* [41], performed a similar study on the $H_2O\cdots Cl_2$ complex and concluded that the photolysis product was a complex between HOCl and HCl with HOCl acting as a base and HCl as an acid. This conclusion was later confirmed by additional codeposition experiments without irradiation.

In 2000, Ramondo *et al.* [42] studied the infrared spectra of Br_2 and H_2O co-deposited on a gold surface, and interpreted the results by comparing to *ab initio* calculations on small clusters. On the ice deposition experiments, they found evidence of the hydrolysis of bromine occurring via $[H_2OBr]^+$. Their theoretical work emphasises the role that polarisation of the Br_2 molecule plays when Br_2 interacts with water. In particular, they conclude that the Br_2 interaction with a H_2O lone electron pair is enhanced for H_2O molecules in hexamer rings compared to an individual molecule.

2.2. *Molecular beam spectroscopy*

In parallel with the matrix isolation experiments, microwave studies on molecular dimers produced with supersonic expansion technology were yielding precise details regarding molecular structure. The first study to reveal electron donation to an interhalogen was performed in 1976 on the complex between HF and ClF, for which the electron donation from the fluorine of HF to the Cl end of ClF is preferred over the hydrogen bonded isomer [43]. Also, the HF···ClF bond length, 2.766 Å, is 0.45 Å shorter than the sum of the two van der Waals radii. Later, Legon and his group performed pulsed-nozzle Fourier-transform microwave spectroscopy studies of a large number of weakly bound dimers, including many water–halogen complexes, to determine the periodic trends in their structure and bonding. Since Legon [44] has comprehensively reviewed this body of work, we will focus on how the studies helped to determine the interaction forces responsible for the surprising stability of these complexes. Their work with a series of different Lewis base electron donors (B) and the hydrogen halides allowed for a definitive characterisation of the hydrogen bond stabilising these complexes. This eventually led to a set of rules, based on *n*-bonding and π-bonding electron pairs, for predicting angular geometries of isolated (i.e., unperturbed by lattice or solvent interactions) hydrogen bonded dimers [45]. This work was followed by an analogous set of studies of Lewis base donation to dihalogen and inter-halogen molecules. In 1998 they proposed that the '*chlorine bond*' [46] has unique properties that deserve special recognition. Later, further studies supported by significant theoretical work prompted them to propose the more general term '*halogen bond*'. This term has been adopted by other investigators who study molecular interactions in condensed phases [47–49].

2.2.1. *The geometry of the $H_2O\cdots X_2$ complex. Planar or effective-planar?*

The ground-state rotational spectra recorded for $X_2\cdots H_2O$ ($X_2 = F_2$ [50,51], Cl_2 [52], Br_2 [53]) complexes, as well as for the $Y–X\cdots H_2O$ series (X–Y = ClF [51], BrCl [54], ICl [55]) can each be characterised as that of an asymmetric prolate rotor. Detailed analysis of the spectroscopic constants, including multiple isotopic substitution studies, confirmed the conclusion from matrix isolation spectroscopy that water acts as a lone pair donor: no H-bonded structures were observed. Furthermore, for the complexes between electron donors and interhalogen molecules, it was found that the more electropositive halogen atom of the interhalogen molecule always attracted the electron donor. Bond lengths for the $H_2O\cdots XY$ complexes are given in Table 1. While comparing the differences, it is useful to remember the van der Waals radii for the oxygen and the halogens [17]: O = 1.52 Å, F = 1.47 Å, Cl = 1.75 Å, Br = 1.85 Å, I = 1.98 Å. For each of the O···X bonds the bond length is significantly shorter than the sum of the van der Waals radii. This is especially true for the examples involving interhalogen molecules.

The general structure of these complexes is shown in Figure 5. A particularly interesting result was that it was possible to fit the experimental data using either a planar structure with $\phi = 0$ (C_{2v}) or a pyramidal one $\phi \neq 0$ (C_s). This indicates a very low barrier for the interconversion between the two geometries. The potential energy as a function of the angle ϕ was experimentally determined for the $H_2O\cdots HF$ complex [56] and the $v = 0$ level was determined to lie only slightly below the barrier. Similar experiments were performed for $H_2O\cdots HF$ [57] and $H_2O\cdots ClF$ [58]. For $H_2O\cdots ClF$ the first two

Table 1. The experimentally derived force constants and the intermolecular distance for the X_2–H_2O complexes and some of the *ab initio* MP/aVDZ dissociation energies of the complexes.

	H_2O–F_2	H_2O–Cl_2	H_2O–Br_2	H_2O–ClF	H_2O–BrCl	H_2O–ICl
k_σ Nm^{-1} [53]	3.7(1)	8.0(1)	9.8(2)	12.1	14.2	15.7
R (O···X) Å [53]	2.719(4)	2.8479(3)	2.8506(1)	2.608(2)	2.7809(3)	2.838(3)
μ D [59]	–	–	–	0.888061	0.519 ± 0.004	1.24 ± 0.02
E_{int} (kcal mol^{-1})	1.27 [51]	2.82 [52]	3.28 [60]	5.07 [51]	4.45 [54]	–

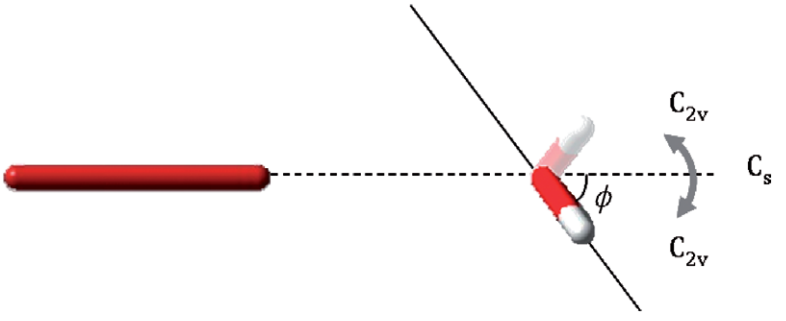

Figure 5. [Colour online] General structure of the X–Y···OH_2 complex. ϕ is the angle formed by the HOH plane and the X–Y···O axis.

vibrational levels are below the potential energy barrier and the equilibrium geometry was confirmed to be a C_s structure. The experimental determination of this barrier was not feasible for all the complexes considered here but was obtained by means of *ab initio* calculations. In most cases the height of the barrier is close to the energy of the first vibrational level, so the structures are *effectively* planar. Exploring the parallelism between the hydrogen halides series and the dihalogens species was one of the goals of these studies and the structural features showed that the interhalogen complexes have a striking similarity with the corresponding hydrogen halides.

2.2.2. *The trends in the stretching force constant*

Although the stretching force constant is not directly related to the bond energy, usually there is a positive correlation between the two properties. So, measuring the halogen bond force constants for a variety of species allows the relative donor–acceptor strength to be compared. In the microwave studies, the stretching force constant, k_σ, for the halogen bonds can be estimated from the measured centrifugal distortion constants. This estimation assumes that the main effect of centrifugal distortion is to stretch the weak bond without significantly affecting other properties of the molecule. For $H_2O\cdots F_2$ Cooke *et al.* [50] found that $k_\sigma = 3.63(7)$ Nm^{-1}. This compares to $k_\sigma \cdots = 1.4$ for Ar···HF and 24.9 Nm^{-1} for $H_2O\cdots HF$, indicating very weak binding for $H_2O\cdots F_2$. Table 1, lists the force constants for each of the studied molecules. The value for $H_2O\cdots F_2$ is unusually small. The value for $H_2O\cdots ClF$ is about half as large as that of the strong hydrogen bond, $H_2O\cdots HF$. It is interesting to note that the force constant for $H_2O\cdots BrCl$ is larger than

that of $H_2O\cdots ClF$, even though the XY dipole moments and the calculated bond energies have the opposite trend. To date, no experimental data has been reported for the $H_2O\cdots I_2$ complex nor for the three of the six possible interhalogen compounds. However, from the observed trends, it is expected that the bond strength for H_2O–I_2 lies between those of $H_2O\cdots Br_2$ and $H_2O\cdots ClF$.

2.2.3. *Charge transfer (XY) and polarisation (X2)*

The fact that interhalogen compounds have permanent dipole moments ranging from 0.4 to 1.95 D explains not only their additional stability but serves as a reminder that electrostatics are an important component of halogen bonding. Davey *et al.* [54,55], analysed the inter- and intramolecular charge transfer in the $H_2O\cdots BrCl$ and $H_2O\cdots ICl$ complexes using a model that analyzes the nuclear quadrupole coupling constants that are quite sensitive to the electric field gradient at that nucleus due to charge transfer and polarisation. The intermolecular charge transfer, $\delta_i e$, and the X–Y polarisation, $\delta_i p$, occurs mainly along the O···X–Y axis. While these effects are not independent of the internal motions of the complex, assuming that the experiment measures the contribution at the equilibrium geometry is a reasonable approximation. For both complexes very small $\delta_i e$ values were found and it was suggested that this is due to the high ionisation potential for water. The polarisation values $\delta_i p$ are five to six times more important than the intermolecular charge transfer. These findings, while not completely unexpected, are important for at least two issues related to halogens in aqueous media: first, it is possible to think that the large polarisation occurring in the X–Y molecules is also occurring in the X–X ones; second, as suggested by several authors in the context of atmospheric chemistry, [42] many-body polarisation may lead to the formation of ionic pairs in the presence of additional water molecules.

3. Theory of halogen bonding

In this section, we will follow the evolution of the understanding of the molecular interactions responsible, not only for the stability of the water–halogen complexes, but also for their observed properties in the gas and condensed phases. This will emphasise the interdependence of theory and experiments and the challenges each faces in achieving a complete description of the important interactions.

3.1. *Early models: The charge transfer era*

The experimental findings on the valence spectra of halogens in different solvents prompted inquiries into the forces that bring together solvent molecules (oxygenated solvents ranging from ethers to alcohols and water) and the halogens. Mulliken's [31] work on this problem convinced him that van der Waals forces were not enough to explain the changes since van der Waals forces are certainly also present in the so-called 'inert solvents'. He strongly suggested that the observed effects occurring in aromatic solvents and oxygenated solvents were a consequence of the changes occurring in the valence region of the halogen. In particular, for the case of R_2O–I_2 the most direct cause of the changes in the spectra (shift and broadening) could only be explained in terms of the transfer of an

electron from the 'lone pair' of the oxygen atom to the halogen molecule leading to a structure in which the iodine molecule attaches to the oxygen atom with its axis perpendicular to the R′RO plane. For both types of solvent, Mulliken invoked a charge transfer complex in which the contribution of at least two resonant structures was proposed. This idea was very much in line with the chemical bonding ideas of the time and was quickly adopted by the chemistry community who adopted this idea as a cornerstone for the charge transfer phenomenon. Mulliken's charge transfer idea was combined with earlier definitions of acids and bases by Lewis [61] and the derived nomenclature of donor–acceptor interactions proposed by Sidgwick [62]. This led to a pause in the investigation into the nature of the interaction between halogen molecules and oxygenated solvent molecules that were equally regarded as a donor–acceptor and/or charge transfer complexes.

Some years later, the diffraction experiments of Hassel [35,63], Hassel and Stromme [64], Hassel *et al*. [65] and Groth and Hassel [66] on the adducts of bromine and 1,4 dioxane and other oxygenated solvents and halogens, showed that the axis of the X–Y bond coincided with the orientation of the orbital containing the lone pair of the solvent molecule. The structure of these systems showed that the intermolecular distances were shorter than the sum of the van der Waals radii, confirming the existence of a strong interaction. However, as he mentioned in his Nobel lecture in 1970: '*the formation of molecular complexes may generally be attributed to a transfer of negative electrical charge from a donor molecule* (*Lewis or Brønsted base*) *to an acceptor molecule* (*the Lewis acid*) *and it had become natural to classify the process involved as a "charge-transfer"* 'interaction' [67]. This statement, sustained the belief that the correct interpretation of the spectroscopic studies of halogens in different environments would invoke charge transfer phenomenon.

3.2. *Development of the halogen bond classification*

The experimental work of Fredin and Nelander [36] in 1973 was accompanied by a set of theoretical calculations aimed at exploring the possible stable structures of the $H_2O\cdots Cl_2$ complex at the complete neglect of differential overlap (CNDO) level. Their findings showed that a Y-shaped structure, in which all the atoms lie in the same plane is, even at this modest theoretical level, more stable than the structure advanced by Mulliken. Furthermore, these calculations showed, as a consequence of the interaction, a large charge polarisation of the chlorine molecule. Two years later, their findings were confirmed by the calculation of the potential energy surface (PES) of the $H_2O\cdots Cl_2$ complex at the self-consistent field (SCF) level with the Stater type orbital, three Gaussian (STO-3G) basis set [68]. This work found that the $Cl\cdots O$ distance is 2.9 Å, 0.6 Å longer than the semi-empirical result and in better agreement with diffraction experiments on related systems. The analysis of the charge distribution in the complex on the minima region of the PES supported their conclusion that polarisation effects on the halogen molecule are considerably more important than the charge transfer, as had already been pointed out by other authors [69,70]. In the early 90 s, McInnis and Andrews [40] used Hartree–Fock calculations to investigate the relative stabilities of the possible products of the H_2O+F_2 photochemically induced reaction in Ar matrices. They studied two possible arrangements for the $H_2O\cdots F_2$ complex, the hydrogen bound ($HOH\cdots F_2$) and what they called the Lewis acid–base ($H_2O\cdots F_2$) type. Even without correlation effects and using

small basis sets (DZP, double zeta polarization), the Lewis acid–base complex, i.e. the oxygen lone pair bonded to the end of F_2 via donation into the σ orbital is more stable than the sideways arrangement, (π-bonded to F_2) by 0.2 kcal mol^{-1} and the hydrogen bonded isomer by 0.5 kcal mol^{-1}. Further support for this geometry of the stable structure was that the shifts predicted by their calculations for the σ bonded complex were in better agreement with their experiment than the other two conformations. Dahl and Roeggen [71] included the correlation effects in the study of F_2, Cl_2 and ClF complexes and using a decomposition scheme of the energy for F_2 found little involvement of oxygen lone pair and large polarisation effects. With these studies, theoretical methods provided strong arguments for revising the picture of halogen–water interactions.

The picture emerging from the combined microwave spectroscopy experiments and theoretical calculations done by Legon's group on a large set of B···X–Y complexes and the similarities found with the analogous H-bonded systems (H_2O···HX) led to the coinage of the 'halogen bond' term to define the interaction appearing between an accepting halogen atom and a Lewis base donor. With this, the long controversy over the importance of charge transfer complexes relative to donor–acceptor interactions was finished. Noting the parallels between hydrogen bonding and the forces responsible for the stability of B···X–Y complexes, Legon defined the halogen bond adapting the IUPAC accepted definition of the formers, i.e. '*The halogen bond is an attractive interaction between a halogen atom X and an atom or a group of atoms in different molecule*(*s*), *when there is evidence of bond formation*' [44]. The properties of this type of interaction can be generalised as:

- The physical forces involved in the halogen bond must include electrostatic and inductive forces in addition to London dispersion forces.
- The atoms Y and X are covalently bound to one another, and B···X–Y is polarised so that the X atom becomes more electropositive (i.e. the partial positive charge δ^+ increases).
- The lengths of the X–Y bond and, to a lesser extent, the bonds involved in B deviate from their equilibrium values.
- The stronger the halogen bond, the more nearly linear is the B···X–Y arrangement and the shorter the B···X distance.
- The interaction energy per halogen bond is greater than at least a few times kT, where T is the temperature of the observation, in order to ensure its stability.

For systems where the Y atom is not a halogen, an equivalent definition had been previously proposed by Metrangolo *et al*. [48] who have recognised the potential utility of this type of interaction in supramolecular chemistry and crystal design, [49,72,73] and also, the model of the σ-hole bonding to explain the origin of halogen bonds. In this model, the electrostatic potential resulting from the three pairs of unshared electrons on the halogen atom X form a negative electrostatic potential around the Y–X axis, leaving a positive 'σ-hole' on the outer most portion of its surface, centred around the same X–Y axis. This σ-hole can interact favourably with negative sites on other molecules, giving rise to halogen bonding [74,75].

As for hydrogen bonds, this new type of interaction opened interesting questions about the structure of the complexes formed, their stabilisation energy, their (intermolecular)

vibrational frequencies and the potential energy and free energy surfaces. The search of reliable answers to some of these questions can be thought of as being approached from opposite extremes; on one side with the study of strongly bound complexes and on the other by the weakest possible ones. We will summarise what can be thought of as the extreme situations for complexes with halogens.

3.2.1. *Halogens in weak interactions*

The weakest interaction found with halogens corresponds to the Rg···X–Y complexes. The interaction is dominated by van der Waals attraction and exchange repulsion and the electrostatic component is negligible. Many combinations of Rg and X–Y have been experimentally studied and many of the PES have been calculated [76]. Although the binding energies are smaller than $1\,\mathrm{kcal\,mol^{-1}}$ ($\sim 100\,\mathrm{cm^{-1}}$), there are still two stable configurations, one linear and the other T-shaped, for each of the complexes. (For Rg···X–Y, there are two linear configurations [77].) It has been found that the linear and the T-shaped configurations have very different spectroscopic and dynamic properties. In spite of looking like a simple model system, from the earliest studies it was clear that the anisotropy of the interaction prevented the transferability of simple empirical potentials for describing the PES. For instance, it has not been possible to obtain diatomic-in-molecule potentials without adjustable parameters [78]. High level *ab initio* calculations are required to extract the subtlety of the interactions. For the electronic excited states, this is still an open problem. The soft potential and the large dispersive nature of the interaction require the use of methods able to recover most of the correlation energy and this usually implies that at least MP4 level is required to get a reasonable idea of the depth of the well. For a description of electronic states different from the ground state, usually the molecular orbitals have to be optimised in the complete active space and the correlation energy calculated by means of multi-reference configuration interaction methods and spin–orbit coupling corrections [78,79]. Although the Rg···X–Y dimers are simpler than the H_2O···X–Y halogen bonded molecules, the insight gained from these studies is useful in moving towards a complete description of halogen bonding.

3.2.2. *Halogens in strong interactions*

There have been many studies of complexes between X–Y molecules and a broad range of Lewis bases (B) [47,74,75,80–96]. An interesting feature of this class of dimers is that, in spite of being weakly bonded, they show all the structural and vibrational spectroscopic features encountered in the case of hydrogen bonding [84,96–98]. Also, the intermolecular distances are consistently shorter than those expected from the sum of van der Waals radii [47,83,91,98].

Karpfen recently reviewed the theoretical results of a large group of complexes, Y–X···NR and C–X···NR and C–H···NR [98]. For the dihalogens and the amines, the Möller–Plesset Pertubation theory (MP2) calculated interaction energies can vary from quite weak, $1.8\,\mathrm{kcal\,mol^{-1}}$ in F_2–NH_3 to quite strong, $14.6\,\mathrm{kcal\,mol^{-1}}$ in the complex BrF–NH_3 ($\mu_{BrF} = 1.422 \pm 0.016$ D). In each of these cases, the X–Y···NH_3 structures had C_{3v} symmetry with the X–Y···N–fragment perfectly linear. The other type of halogen

bonds, C–X···B or C–X···H–C are more weakly bonded. As a model of this latter group, Riley and Hobza [99] used refined *ab initio* calculations for the system of formaldehyde bonding to the halomethane series (Cl, Br and I) and studied the nature of the interaction by means of the symmetry adapted perturbation theory (SAPT). The values of the interaction energies for these complexes are in the range of 1.12–2.25 kcal mol^{-1} for R···Cl to R···I. In this case the R–X···O– fragment is not linear, with angles ranging from 167° to 173°. They found a large dispersive character (50–70%) for the C–X···H–C interactions that explains the differences from the analogous C–O···H–C hydrogen bonded complexes, for which the main contributions are the electrostatic interactions. Thus, for these examples, the nature of the interaction is modulated by the electronegativity of the group bound to the donor halogen atom (X); the more electronegative the group or atom (Y) bound to X, the stronger the electrostatic component of the interaction, and the greater the similarity to hydrogen bonding.

It is also useful to consider the interactions between water and the hydrogen halides. The hydrogen bonds formed in these systems, from the neutral H–X···H–X and H–X···H_2O to the charged cases, have received much attention [45,100–102] These studies, driven by many different interests, from gas phase behaviour and the connection to atmospheric chemistry to condensed phase simulations interested in shedding some light on fundamental acid dissociation, provide a wealth of information for these complexes [103–117]. The dissociation energies calculated place the neutral examples among the moderately strong H-bonds. There are three possible configurations for a water molecule bonded to a hydrogen halide: two hydrogen bonded structures, H_2O···H–X and H–X···HOH; and a halogen bonded one, H_2O···X–H. Only the first one has been thoroughly studied because, as expected, it is the most stable. Nonetheless, the other two

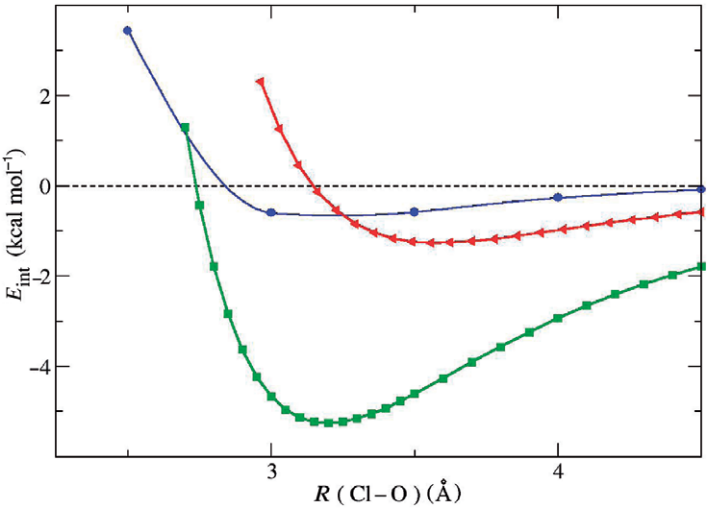

Figure 6. [Colour online] Interaction energy curves for HCl···H_2O calculated at the MP2/aug-cc-pVTZ level. All values were corrected from the BSSE error using the full counterpoise correction. The green line (■) is for the HB H_2O···HCl conformer. The red line (▲) is for the H–Cl···HOH conformer and blue line (●) is for the XB H_2O···Cl–H conformer.

conformations lead to minima on the PES and deserve analysis. In Figure 6 the interaction energy curves for the H_2O–HCl complexes are shown, the –O···H–Cl minimum is at r(O–Cl) = 3.192 Å and has a $E_{int} = -5.79\,kcal\,mol^{-1}$, the –Cl···HOH curve has the minimum located at r(O–Cl) = 3.513 and $E_{int} = -1.75\,kcal\,mol^{-1}$. In contrast with the first hydrogen bonded structure that has a linear Cl–H···O fragment, in this case the O···Cl–H fragment forms an angle of 142.7. The exact position of the third conformation minima is not known but its existence was confirmed by checking that coupled-cluster with single, double and perturbative triple excitations (CCSD(T)) methods predict a point in the minimum region of the curve as an attractive interaction [118]. Due to the strong acid character of HCl, it is expected that the other two minima might not be very relevant in the gas phase chemistry. However, they are a good example of the wide variety of interactions in which halogen atoms may be involved.

The long controversy on the physical nature of hydrogen bonds, more specifically, the degree of electron delocalisation in these systems [119–122] has also been discussed for the halogen bonds [92,98,99] We address this issue in order to better understand the persistence of the charge transfer idea associated with the nature of halogen bonds. Any covalent character of intermolecular forces inherently involves electron delocalisation and often involves partial charge transfer. For hydrogen bonds it is possible to arrive at different conclusions regarding the extent of charge transfer content depending on the scheme used. Morokuma-type and perturbation expansions yield smaller contributions, ~20%, than natural bond orbital (NBO)-like methods, ~60%. The origin of the differences between these methods depends on the orbital approach used to define them and is both complicated and convoluted. This has been discussed in detail by Martín Pendás *et al.* [122] for hydrogen bonding.

The charge transfer occurring for halogen bonded complexes has been evaluated with several different methods. Each of these suggests that the total intermolecular charge transfer is small, but non-zero, ranging from 0.005 to 0.050 electron, always in the Y–X ← B direction such that the B atom loses charge that is gained by the X [93,99,123,124]. This small amount of charge transfer has been confirmed by other calculations using HF and correlated methods and very different basis sets [80,125,126].

The SAPT method has been the most commonly used method to gain increased understanding of the nature of the halogen bond interaction. In this approach, six terms contribute to the interaction energy: $E_{int} = E^{(1)}_{pol} + E^{(1)}_{exch} + E^{(2)}_{ind} + E^{(2)}_{ex-ind} + E^{(2)}_{disp} + E^{(2)}_{ex-disp}$, and these can be combined in the form of the physically recognisable interactions as: the electrostatic term, $E_{ELST} = E^{(1)}_{pol}$; the induction term, $E_{IND} = E^{(2)}_{ind} + E^{(2)}_{ex-ind}$; the dispersion term, $E_{DISP} = E^{(2)}_{disp} + E^{(2)}_{ex-disp}$ and the exchange term, $E_{EXCH} = E^{(1)}_{exch}$. There is no explicit charge transfer contribution but it forms part of the induction and the second-order term of exchange – induction [121]. Several conclusions can be drawn from the relative contribution of this term in different studies: for the weakest interactions, C–X···B [99], induction accounts from 7%, 10% and 14% of the total attraction going from X = Cl to I; for X–X···OH_2 it is 9% for Cl_2 and 10% for Br_2 [123] and for Y–X···OH_2 it is 11% for FCl···FH and 13% for FCl···OH_2 [93]. This confirms that charge transfer is not the driving force for the stability of these complexes and is in good agreement with other calculations and with the analysis of microwave spectra. In general, the strongest interactions with halogens result from a significant electrostatic contribution due to the presence of a permanent dipole moment in the Lewis base entity with the dipole of the

halide molecule X–Y ($X \neq Y$) or its quadrupole ($X = Y$). The stability of the less strongly halogen bound complexes is largely due to dispersion.

The ensemble of rotational spectroscopic results and some of the theoretical calculations on different B···X–Y systems have already been reviewed [44,46,47,53,98]. However, recently, more refined studies have examined a wider variety of properties for this system and have led to a better understanding of the nature of the interactions. The systematic analysis of these results will be presented below, following a section on recent experimental results.

4. Spectroscopy of halogen hydrates

We became interested in halogen clathrate hydrates when we learned of the growing importance of methane clathrate hydrate. In short, there is more methane stored in hydrate deposits than all other geological hydrocarbons combined [127–129]. This methane provides both the opportunity of providing energy for the economy far into the future and the danger of run-away global warming [130]. Reading about methane hydrate led us to the halogen hydrate literature and the surprising fact that there had been no UV-vis spectroscopic studies of these very interesting substances. Our hope is that by understanding halogen-hydrates in greater detail, we may also advance the understanding of hydrocarbon hydrates for which the UV-vis tool is not applicable. To this end, we have reproduced aqueous solution phase spectra for Cl_2, Br_2 and I_2, and have recorded the first UV-vis spectra for each of the molecules in a clathrate hydrate environment. In addition, Raman and ultrafast relaxation experiments have been performed to explore the cage–guest interactions and the dynamics of recombination for Br_2 photo-excited over the dissociation threshold in aqueous solution and clathrate hydrate cages. A selection of the UV-vis spectra are shown in Figure 7, and a summary of the results are given in Table 2. We discuss the results for bromine first, since it is the molecule for which we have the most detailed results.

4.1. *Bromine clathrate hydrates*

Before reviewing the bromine hydrate spectroscopy, we briefly discuss a fascinating phenomenon we discovered regarding bromine hydrate crystal growth. As mentioned above, at one time it was postulated that the wide range of bromine hydrate stoichiometries that had been observed might be due to the fact that there is more than one crystal structure [25]. The 1997 study of Udachin *et al.* [23] appeared to put that speculation to rest with the observation that the TS-I crystal structure results from a wide variety of preparation mixtures. (Crystal notation was discussed in Section 1.1.) However, we have now observed at least three different crystal structures for bromine hydrate as revealed by their spectra. The apparatus and details of the experiment are given in Ref. [25]. Here we provide a brief summary of some of the important observations.

After loading an emulsion formed by melting a polycrystalline bromine hydrate sample into the cell, the emulsion was quickly cooled to –20°C to form seed crystals. Upon heating above 0°C the ice melted, revealing that small bromine clathrate crystals were formed. These crystals were stable to +5.8°C, the melting point of bromine hydrate in the tetragonal crystalline form, TS-I. Careful cycling of the temperature around the hydrate

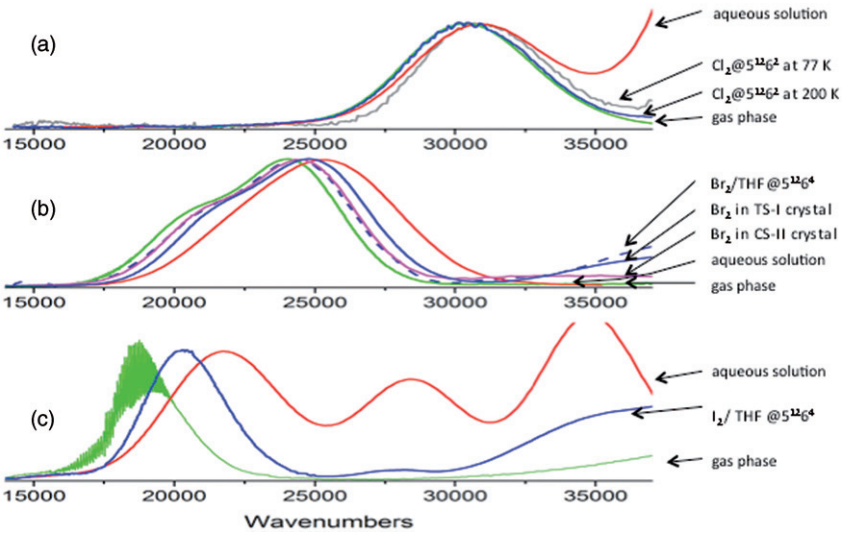

Figure 7. [Colour online] Spectra of (a) chlorine, (b) bromine, and (c) iodine in various environments. In each case the green curve is the gas phase spectrum and the red curve is for an aqueous solution. (a) For chlorine, the blue curve is mainly due to chlorine in $5^{12}6^2$ cages at 200 K, the gray curve was recorded for the same sample at 77K. (b) For bromine, the blue curve is for the TS-I single crystal sample, the magenta curve is for the CS-II crystal, and the dark blue dashed line is for bromine in $5^{12}6^4$ cages of THF clathrate hydrate. (c) For iodine the blue curve is the previously reported spectrum for iodine substituted into the $5^{12}6^4$ cages of THF clathrate hydrate.

melting point resulted in a single seed crystal in the optical path. This crystal was then allowed to grow for four days at +4.8°C, and formed an optical quality crystal that filled the 10 μm space between the windows and had a diameter of ~0.5 mm. Under these conditions the crystal is expected to be nearly stoichiometric. The sample was then quickly cooled to –20°C in order to freeze the surrounding water and the spectrum shown as the blue trace in Figure 7(b) was recorded. This spectrum for this crystal was very similar to that previously reported for polycrystalline samples.

After obtaining the spectrum of the TS-I bromine hydrate as described in the preceding paragraph, the sample was warmed above 0°C to melt the liquid water around the crystal and then the temperature was slowly lowered to −9°C. As the temperature reached −5°C the TS-I crystal started to disintegrate and a new solid phase started to grow on its surface. It is important to note that, even though the temperature is below 0°C at this stage of the experiment, the bromine hydrate crystals are immersed in bromine saturated liquid water. If left alone, these new crystals had a feather-like appearance and grew until the original seed crystal was completely devoured. If these new crystals are heated slowly, they revert back to the TS-I crystals above −5°C; but if they are heated moderately rapidly, they remain metastable until their melting point of 4°C. By careful manipulation of the temperature, it is possible to find a seed crystal of the new structure and melt the surrounding solid so that the seed may grow. After 24 h such a crystal was of optical

Table 2. Band maxima of the valence electronic bands of halogens in different environments compared to the gas phase.

	Chlorine[a]		Bromine[b]				Iodine[c]	
Environment	ω_{max}[d] (cm^{-1})	$\Delta\omega_{max}$[e] (cm^{-1})	ω_{max} · C–X (cm^{-1})	$\Delta\omega_{max}$ (cm^{-1})	ω_{max} · B–X (cm^{-1})	$\Delta\omega_{max}$ (cm^{-1})	ω_{max} (cm^{-1})	$\Delta\omega_{max}$ (cm^{-1})
Gas phase	30,300	0	24,270	0	20,830	0	18,870	0
C_6H_{12} solution	–	–	24,160	−120	20,760	−70	19,120	250
CCl_4 solution	30,180	−120	24,390	120	20,920	90	19,360	490
CH_2Cl_2 solution	30,830	530	24,720	450	21,300	470	19,800	930
$5^{12}6^2$ cage	30,300	0	25,150	880	21,720	890	–	–
$5^{12}6^4$ cage (doped THF hydrate)	–	–	24,630	360	21,190	360	20,310	1440
$5^{12}6^4$ cage (single crystal)	–	–	24,710	440	21,270	440	–	–
Aqueous solution ($T = 293$ K)	30,850	550	26,000	1730	22,590	1760	21,690	2820
Amorphous ice ($T = 120$ K)	–	–	25,980	1710	22,670	1640	21,870	3000

Note: [a]The chlorine spectrum is dominated by the $\mathbf{X} \rightarrow \mathbf{C}$ transition.
[b]The bromine spectrum has been deconvoluted into the $\mathbf{X} \rightarrow \mathbf{C}$ and $\mathbf{X} \rightarrow \mathbf{B}$ transitions. See [24] for details.
[c]The iodine spectrum is dominated by the $\mathbf{X} \cdots \mathbf{B}$ transition. See [26] for details.
[d]ω_{max} is the position of the absorption maximum, $\pm 50\,cm^{-1}$.
[e]$\Delta\omega_{max}$ is the shift of the absorption maximum from the gas phase value.

quality and large enough to record its spectrum. The UV-vis spectrum of one such crystal is shown in Figure 7(b). This spectrum is very similar to that previously recorded for polycrystalline tetrahydrofuran (THF) clathrate hydrate samples with small amounts of bromine doped into the resulting $5^{12}6^4$ cages. On this basis, we conclude that the new crystals have the CS-II crystal structure. Although we are eager to confirm this conclusion with X-ray analysis, the circumstantial evidence for our conclusion is very strong.

4.1.1. *UV-vis spectra of bromine hydrates*

Next, we turn to an analysis of the spectra. For Br_2, we have recorded the UV-vis spectrum in amorphous solid water, polycrystalline TS-I and CS-I samples and CS-II and TS-I single crystals for comparison to the gas phase, aqueous solution and other solvents. We have also been able to record the Raman spectra for CS-II and TS-I single crystals. As illustrated in Figure 7(b), the gas phase and aqueous environments provide two limiting cases for the UV-vis spectra. As reviewed above, the gas phase spectrum, recorded at low resolution is dominated by the relatively strong $\mathbf{X} \rightarrow \mathbf{C}$ transition whose peak is at $24{,}270\,cm^{-1}$. A weaker side band is due to the $\mathbf{X} \rightarrow \mathbf{B}$ transition that would show resolved structure under higher resolution. In aqueous solution, the two bands are broadened and the $\mathbf{X} \rightarrow \mathbf{B}$ side band blends into the stronger $\mathbf{X} \rightarrow \mathbf{C}$ transition. Although deconvolution of such blended bands is inherently imprecise, our best estimate is that the $\mathbf{X} \rightarrow \mathbf{C}$ transition is shifted $1730\,cm^{-1}$ to the blue and broadened by $1100\,cm^{-1}$ in going from the gas phase to aqueous solution. In amorphous ice, the Br_2 spectrum is very similar

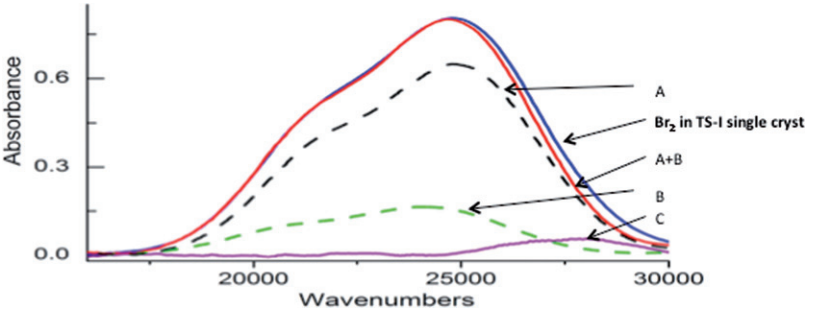

Figure 8. [Colour online] The blue curve is the bromine hydrate TS-I single crystal spectrum. The dashed black curve (A) is the proposed CS-I spectrum (adjusted to be 80% as intense as the TS-I spectrum) from a polycrystalline film and dominated by bromine in $5^{12}6^2$ cages. Note that, even though the dashed curve is for a polycrystalline sample, its width is less than that of the TS-I single crystal, as evidenced by the better definition of the two bands. The dashed green curve (B) is the same as the black curve (A), except that it is shifted to the red by 700 cm^{-1} and adjusted to be 20% as intense as CS-I spectrum. The sum of the black (A) and green (B) curves yields the red curve, which closely fits the observed single crystal spectrum except in the UV wing. The purple curve (C) is the residual of the fit. The close reproduction of the TS-I spectrum by A + B convinces us that (A) represents bromine in the $5^{12}6^2$ cages while B represents bromine in the $5^{12}6^3$ cages.

to that of aqueous solution: the blue shift is 1710 cm^{-1} and the broadening is 700 cm^{-1}. However, the band for Br_2 in a $5^{12}6^4$ cage of a CS-II clathrate hydrate is closer to the gas phase than to the aqueous solution limit. In this case the band is blue shifted only 440 cm^{-1} and it is broadened by only 100 cm^{-1}. Although many effects contribute to these phenomena, we believe that the most important single effect is that the water molecules in the clathrate hydrate cages are fully hydrogen bonded, so the oxygen non-bonding electron pairs are not available for halogen bond formation with the Br_2 molecule guests. Qualitatively, the inside of the hydrate cage is more like non-interactive solvent than like aqueous solution.

The spectra for Br_2 in TS-I single crystals, is about halfway between that of the gas phase spectrum and that of aqueous solution. The peak of the spectrum is blue shifted by 880 cm^{-1}, twice that of the CS-II crystals but half that of aqueous solution. The effective diameter (cage diameter minus the oxygen atom van der Waals diameter) of the $5^{12}6^4$ cages of the CS-II crystals is 6.6 Å. This can be compared with the van der Waals length of a Br_2 molecule, 6 Å. In the TS-I crystals, 80% of the bromine molecules are in $5^{12}6^2$ cages with an effective long diameter of 5.7 Å. While the water molecules of these smaller $5^{12}6^2$ cages are equally completely hydrogen bonded as they are in the larger $5^{12}6^4$cages, the tighter fit around the Br_2 molecules results in a stronger perturbation of the spectrum.

In addition to recording the spectra of bromine in TS-I and CS-II hydrate single crystals, we are convinced that we have also obtained spectra for polycrystalline CS-I films. The data used to support this conclusion is illustrated in Figure 8, which shows the spectrum of TS-I single crystals, compared to those of a rapidly grown polycrystalline film. Surprisingly, the spectrum of the polycrystalline film is actually slightly less broad than that of the single crystal. It is also slightly more blue shifted. Remember, the TS-I single crystals are composed of 5^{12}, $5^{12}6^2$, and $5^{12}6^3$ cages in a 10:16:4 ratio. Since Br_2 molecules only fit in the two larger cage types, 80% of them are in $5^{12}6^2$ cages, 20% in $5^{12}6^3$ cages.

These two types of cages result in inhomogeneous broadening, the 20% of the spectra due to the $5^{12}6^3$ cages is less blue shifted than those into the $5^{12}6^2$ cages. Although we have not been able to separately measure the spectra for $5^{12}6^3$ cages, we may expect them to be more like those of the $5^{12}6^4$ cages than the $5^{12}6^2$ cages, since the effective long diameter of $5^{12}6^3$ cages is 7 Å, even longer than the diameter of the nearly spherical $5^{12}6^4$ cages. In a CS-I film, bromine molecules would only fit in $5^{12}6^2$ cages. One type of cage results in a narrow spectrum which is more blue shifted since the cage is small.

Assuming that the individual bands of Br_2 in $5^{12}6^3$ cages have the same shapes as those of Br_2 in the $5^{12}6^2$ cages, but less blue shifted, we construct the TS-I spectrum by taking 80% of the polycrystalline film spectrum, and adding 20% of the same spectrum red shifted by 700 cm^{-1} to represent the $5^{12}6^3$ cages. Note that the resulting trace is very similar to the TS-I spectrum except on the UV edge. In particular, the 'red shoulder' region where the $\mathbf{X} \rightarrow \mathbf{B}$ and $\mathbf{X} \rightarrow \mathbf{C}$ bands overlap is very closely reproduced. Again, while not a direct structure determination, the circumstantial evidence is strong for the conclusion that the black-dashed trace represents the spectrum of a CS-I polycrystalline film. In particular, we believe the narrow width of the spectrum is a compelling argument that only a single cage type contains bromine molecules in this material. Parameters that characterise the spectra discussed above, as well as that for the other halogen hydrates, are collected in Table 2.

4.1.2. *Raman spectra of bromine hydrate single crystals*

In addition to the UV-vis spectra, Raman spectra were obtained for the TS-I and CS-II bromine hydrate crystals [24]. The two spectra are shown in Figure 9. The top traces are the raw spectra, the middle traces are the background scattering recorded in the vicinity near the crystals and the bottom traces are the synthetic fit to the difference between the raw spectra and the background. Note in particular the long resonance Raman progression. Overtones up to $\nu = 9$ are easily observed. The progression would be even longer if not for the interference of the water O–H stretching vibrational modes. Although the two spectra are similar, close inspection reveals that they are distinctly different. Careful fitting using a Birge–Sponer analysis taking into account the isotopic composition yields the vibrational frequencies and anharmonicities listed in Table 3. $\omega_e = 321.2\,cm^{-1}$ from $^{79}Br_2$ in the $5^{12}6^2$ cage of the TS-I crystal and 317.5 cm^{-1} in the $5^{12}6^4$ cage of the CS-II crystal. These values can be compared to $\omega_e = 323.3\,cm^{-1}$ for gas phase $^{79}Br_2$ and $\omega_e = 306\,cm^{-1}$ for Br_2 in an aqueous solution. The value in aqueous solution is less precisely known since only the fundamental band can be observed: there is no resonant Raman progression.

The vibrational frequency of bromine is less perturbed in the smaller $5^{12}6^2$ cage than in the larger $5^{12}6^4$ cages, and it is not nearly as perturbed in either of the hydrate solids as it is in aqueous solution. Again, we believe the large shift in aqueous solution reflects the strong halogen bonding interaction between the bromine and water molecules. The usual interpretation for differences in the vibrational red shift for molecules embedded in hydrate cages is that the large cage exerts a stronger pull on the atoms of the guest molecule [131]. This is consistent with the data for bromine, but a complete analysis will necessarily involve a complicated combination of effects. In particular, we expect that polarisation of the bromine by the neighbouring water molecules will play an important role.

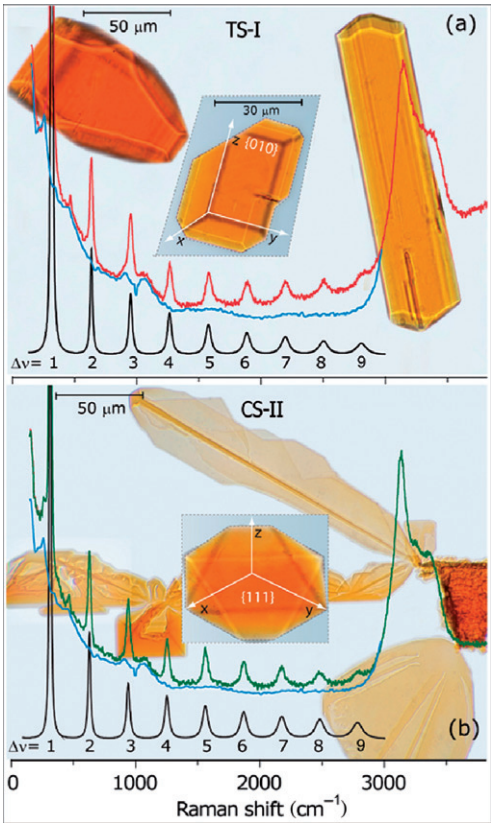

Figure 9. Single crystals and resonance Raman spectra of two different structures of Br_2 hydrate: (a) TS-I, with a space group $P4_2/mnm$, (b) CS-II, with a space group $Fd3m$. The spectra were recorded using a confocal Raman spectrometer with laser excitation at 532 nm, resonant with valence electronic transitions of Br_2. Shown are the experimental spectra of the single crystals (top), the background spectra recorded in the vicinity of the crystals (middle) and the synthetic spectra using the extracted parameters (bottom). The effective temperature of the sample in the focal spot was approximately $-10°C$ due to heating of the sample with the excitation laser. The broad feature at $\sim 3200\,cm^{-1}$ belongs to the OH stretching vibration of the water lattice. Reproduced, with permission, form ref. [25].

Table 3. Vibrational frequencies and anharmonicity constants for chlorine, bromine and iodine in clathrate hydrate cages and in aqueous solution.

	Chlorine		Bromine		Iodine	
Environment	ω_e[a]	$\omega_e x_e$[b]	ω_e[a]	$\omega_e x_e$[b]	ω_e[c]	$\omega_e x_e$
Gas phase	559.7	2.67	323.3	1.06	214.5	0.61
$5^{12}6^2$ cage	–	–	321.2	0.82	–	–
$5^{12}6^4$ cage	–	–	317.5	0.7	214	≤ 0.61
Aqueous solution	538 [135]	–	306	–	–	–

Note: [a]ω_e is the harmonic frequency constant, $\pm 0.1\,cm^{-1}$, $^{35}Cl_2$ and $^{78,81}Br_2$.
[b]$\omega_e x_e$ is the anharmonicity constant, $\pm 0.05\,cm^{-1}$.
[c]$\pm 1\,cm^{-1}$.

4.1.3. *Geminate recombination dynamics for bromine in clathrate cages*

Goldschleger *et al*. performed femtosecond transient grating experiments to study the dynamics of bromine atom recombination after photodissociation [132]. Photodissociation was achieved using a 70 fs pulse at 530 nm to excite the **B** ← **X** transition above the dissociation limit. Recombination on the long lived **A**/**A**′ state curves was monitored by a second 70 fs pulse at 400 nm, which excited the recombined atoms to the ion pair states. The results for bromine in aqueous solution are shown in Figure 10. The time dependence is a single featureless peak (other than the scattered light at $t = 0$) that indicates recombination on the ~1 ps time scale followed by the decay of the **A** states on the several ps time scale.

Figure 11(a) shows the data for the $5^{12}6^2$ cages. In this case the data reveals distinct coherence. The first recombination maximum occurs at 360 fs, and coherent quantum beats occur at 600 and 840 fs. The time for initial recombination is taken to correspond to the bromine atoms reflecting from the cage walls. Note that this time is ~1/3 that in aqueous solution. That the recombination is highly coherent implies that this reflection occurs directly, with little difference between the recombination times of bromine atoms in the ensemble of cages being interrogated. Again, this is in contrast to the incoherent recombination in aqueous solution. The beats correspond to a vibrational period of 240 fs, which corresponds to a frequency of 140 cm^{-1}, somewhat smaller than the value of the **A** state in the gas phase, 153 cm^{-1}. If the cage is only mildly perturbing the **A** state potential, this implies that the molecule is already close to the bottom of the **A** state well in 0.5 ps, having dissipated 4500 cm^{-1} of kinetic energy.

For recombination in the $5^{12}6^4$ cages, Figure 11(b), the coherence is less distinct, the initial recombination takes longer, 490 fs, and the recurrence time is 290 fs. The longer recombination time compared to that in the $5^{12}6^2$ cages is attributed to the longer recombination pathway in the larger cage. Note, however, that recombination still occurs twice as quickly in the $5^{12}6^4$ cage as in aqueous solution. The coherence, which in the

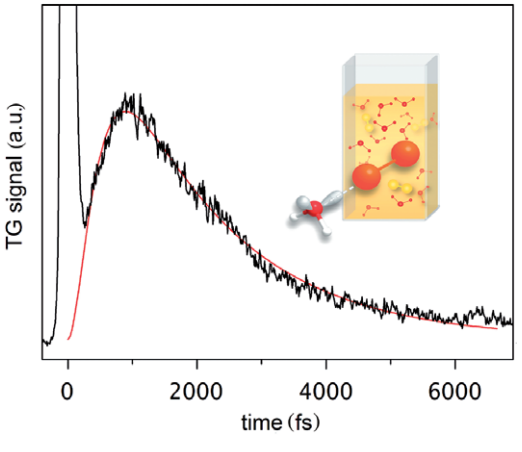

Figure 10. [Colour online] Transient grating signal obtained for: bromine in liquid water (black trace) recorded at $T = 263$ K. The $t = 0$ signal is the response limited non-resonant background. The signal at positive time is due to the geminate recombination of Br_2 on the A/A′ surfaces. The decay of the signal is due to population transfer to the ground state. The red trace is the three-exponential fit, which accounts for build-up subject to induction and decay. Reproduced, with permission, from ref. [132].

$5^{12}6^4$ cages is decreased due to greater dispersion of the recombinative trajectories, is also intermediate between the smaller $5^{12}6^2$ cages and aqueous solution. The longer vibrational period in the $5^{12}6^4$ cages compared to the $5^{12}6^2$ cages has two possible explanations. First, it could be that the bromine atoms lose less kinetic energy before the recombination is measured. This seems unlikely. A second explanation for the lower vibrational frequency is that the **A** state potential is broader in the larger cage. This possibility is supported by the Raman measurements of the ground state frequencies as a function of cage size.

The data sets reviewed above were fitted to a kinetic model to obtain the mean rebound times and the dispersion in the rebound times. The mean rebound times are 300, 400 and 555 fs for $5^{12}6^2$ cages, $5^{12}6^4$ cages and aqueous solution, respectively. The relative values for the two cages is not surprising, and serves to further the assignment of the CS-II crystal that was previously based on electronic spectroscopy, Raman spectroscopy and crystal morphology. The much longer rebound time for aqueous solution is quite interesting.

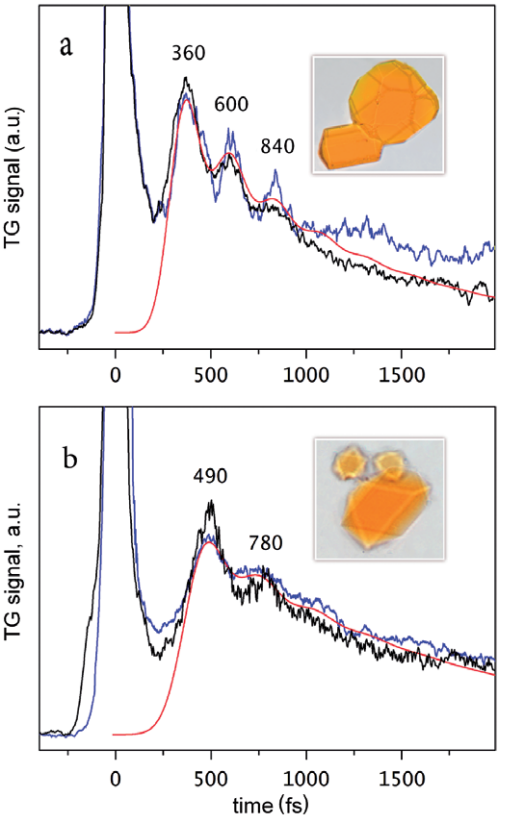

Figure 11. [Colour online] Transient grating signals obtained for: bromine in TS-I (top) and CS-II (bottom) single crystals recorded at $T = 263$ K. The $t = 0$ signal is the response limited non-resonant background. The signal at positive time is due to the geminate recombination of Br_2 on the A/A′ surfaces. The decay of the signal is due to population transfer to the ground state. The quantum beats indicate that recombination in the two crystals is coherent, as discussed in the text. Reproduced, with permission, from ref. [132].

One might think that liquid water would form a close fitting shell around bromine. This expectation is supported by the larger shifts in the valence electronic spectra and ground state Br_2 vibrational frequencies in aqueous solution compared to the hydrate cages. The long rebound time for aqueous solution may be due to the fact that the less specific hydrogen bonding pattern of a liquid makes it more difficult to dissipate kinetic energy. The dispersion in the rebound times, $\sigma = 70$, 100 and 400 fs for $5^{12}6^2$ cages, $5^{12}6^4$ cages and aqueous solution, respectively, is again as expected for the respective cages and perhaps surprisingly large for liquid water. Of course, in liquid water it is possible for water molecules to get between the two bromine atoms to inhibit bromine recombination. Clearly, this is a system ripe for simulation. It would also be fascinating to measure the temperature dependence of the cage recombination dynamics. The above results were obtained at 263 K.

Transient grating measurements were also carried out for bromine trapped in amorphous ice at 120 K for excitation below the **B** state dissociation limit using 550, 536 and 524 nm excitation pulses. Since no dissociation occurs, the atoms stay on the **B** state curve and electronic coherence is prompt. Remarkably, the quantum beats almost immediately (within a vibrational period) correspond to the **B** state $v = 0$ vibrational frequency. This implies that $>1000\,cm^{-1}$ of excitation energy is dissipated during the first vibrational period. Although the appearance of the first coherence peak is longer, 168 fs, for 524 nm excitation than for 550 nm excitation, 134 fs, the following quantum beats have the same period for the two excitation energies. Note that the energy difference between these pulses is $900\,cm^{-1}$. The remarkable ability of amorphous ice to quench vibrational motion is also evident in its ability to quench electronic excitation. The **B** state lifetime measured in this experiment is 1.5 ps, compared to 8 μs in the gas phase, a difference of over six orders of magnitude. The asymmetric environment of amorphous ice is remarkably efficient for quenching this particular excited state. Again, this system is ripe for simulation.

4.2. *Spectroscopy of chlorine clathrate hydrate*

To date, we are yet to obtain spectra for chlorine hydrate single crystals. The technique we used for bromine hydrate does not work for chlorine because the vapour pressure of chlorine hydrate is significantly larger than that of bromine hydrate. We hope to solve this technical problem in the near future. In the meantime, we report spectra for polycrystalline films of chlorine hydrate. These samples were grown from water and gaseous chlorine on a surface of a conventional 10 mm × 10 mm quartz cuvette. The cuvette had a Teflon stopcock to contain the chlorine gas. The crystallisation process was initiated on a cuvette wall by applying dry ice above the water level. After chlorine and water condensed on the inner surface forming a thin hydrate film of a pale green colour, the cuvette was transferred to a quartz Dewar for spectroscopic measurements. The spectra were recorded at ~200 and at ~77 K [133].

The spectrum for chlorine hydrate recorded at 200 K is shown in Figure 7(a). For the preparation conditions we used, we expect that most of the chlorine molecules that contribute to this spectrum are trapped in the larger $5^{12}6^2$ cage of the CS-II hydrate. This spectrum is very similar to the low-resolution spectrum of gas phase chlorine, also shown in Figure 7(a). However, when the temperature is dropped to 77 K, the spectrum shifts

$500\,cm^{-1}$ toward the blue and is very similar to the spectrum of aqueous chlorine solution (to which a small amount of NaCl is added to suppress HOCl formation). These results are reproducible and were observed with several different samples. Our speculative interpretation is that at 200 K the trapped chlorine is mobile and, on average, does not interact in any specific way with the cage walls. When cooled to 77 K the chlorine may localise, and interact with the cage walls about as strongly as it does with liquid water. Note that the width of the hydrate spectrum is similar to that of gas phase chlorine, independent of temperature, while that of aqueous solution is significantly broader. We infer that there is little inhomogeneous broadening of the hydrate spectrum at either temperature. Clearly, we need to obtain spectra for well-defined crystals. We also plan to study the Raman spectrum and X-ray diffraction pattern as a function of temperature to complement the current results.

4.3. *Spectroscopy of iodine in clathrate hydrate cages*

To our knowledge, no one has succeeded in growing iodine hydrate single crystals. We recorded the spectra of iodine molecules trapped in $5^{12}6^4$ cages by growing THF hydrate polycrystalline films doped with a small amount of iodine (I_2 : THF ≈ 0.001) [26]. The resulting spectrum is shown in Figure 7(c). The peak of the iodine spectrum in hydrate cages, $20{,}310\,cm^{-1}$, is about halfway between that of gas phase iodine, $18{,}870\,cm^{-1}$ and that of aqueous solution, $21{,}690\,cm^{-1}$. As for bromine and chlorine, the width of the spectrum in the hydrate is considerably narrower than that of aqueous solution: full width at half maximum (FWHM) $= 3060\,cm^{-1}$ in the gas phase, $3360\,cm^{-1}$ in the hydrate, $4500\,cm^{-1}$ in aqueous solution. Note that the spectrum for aqueous solution has a strong band centred at $28{,}000\,cm^{-1}$. This is due to an intense absorption by I_3^-. Formation of the hydrate shifts the disproportionation equilibrium back toward I_2, so the I_3^- band is very weak in the hydrate spectrum. We expect that it would be completely missing in single crystal spectra.

4.3.1. *The Raman spectrum of the iodine doped THF hydrate*

The Raman spectrum of iodine in doped THF hydrate is not as clean as that of the bromine hydrate crystals since there is an overlapping spectrum of THF. However, a clear progression is observed which allows the extraction of $\omega_e = 214\,cm^{-1}$ for the I_2 stretching vibration, hardly shifted from that of gas phase I_2. In this respect, I_2 in the $5^{12}6^4$ cages is similar to Br_2 in the $5^{12}6^2$ cage, the perturbation of the ground state stretching force constant is small. An interesting question is whether this reflects a small perturbation of the entire ground state curve or whether there is a cancellation of competing effects for stretching and compressing the bond.

Senekerimyan *et al.* [134] performed ultrafast four wave mixing and transient grating spectroscopic studies of iodine doped amorphous water films formed by co-deposition at 128 K. Prior to annealing, the sample is expected to be similar to aqueous solution, except that the overall density is lower. This expectation is supported by the absorption spectrum that is quite similar to that of aqueous solution. In the highly anisotropic environment of amorphous ice, no electronic coherence would be expected. However, the high intensity radiation associated with the ultrafast measurements may induce local annealing.

They were able to observe time-dependent changes in local structure and compare them to those achieved by annealing to 155 K. When different spots of the sample were studied, different types of electronic coherence were observed.

Two limiting types of sites were distinguished. One type of site, in which the coherences were only observed on the ground electronic state, were interpreted to be less asymmetric than those of liquid water, but still rather asymmetric. The coherences indicated that the iodine molecules in these sites were highly polarised by the water's nearest neighbours. In the other limiting case, iodine coherences could be observed for the **B** excited state. This was taken to reveal that the sites for these iodine molecules were highly symmetric, similar to the environment within a clathrate cage. A particularly interesting observation for these sites was that the vibrational period increases with time. This was interpreted as indicating that the iodine vibrational motion serves to push the cage walls further apart. Although no rebound was observed on the time scale of the coherent motion, ~2 ps, it was stated that the cages must return to their original size between sets of laser pulses, ~1 ms. Since electronic coherence is a clear indication that the environment surrounding the iodine molecules is more symmetric than that of liquid water, these experiments hold out the promise that one might be able to study the conversion from iodine doped amorphous ice to enclathrated iodine in real time. Senekerimyan *et al.* [134] propose that the changes in the iodine vibrational frequency and valence electronic spectrum can be understood using a diatomic-in-molecule analysis in which the water molecules induce mixing between the I_2 valence states and ion-pair excited states.

5. Summary of halogen–hydrate spectroscopy

Above, we reviewed the spectroscopy of each of the halogen molecules in hydrate cages without drawing too many comparisons between the three. This section will be devoted to such comparisons. The data behind this comparison is summarised in Tables 2 and 3. Starting with the shift of the valence electronic excitation bands upon solvation in water the differences are dramatic: 550 cm^{-1} for Cl_2, 1730 cm^{-1} for Br_2 and 2820 cm^{-1} for I_2. Clearly, the trend is as expected since the water–halogen dimer bond energies and the halogen polarisabilities are in the same order. Finding a quantitative explanation for these large differences would be a significant accomplishment. We suspect that a key issue is how effective the respective halogen bonds are in competing with water–water hydrogen bonds in the liquid. It is also interesting that for Br_2 in the $5^{12}6^2$ cages and I_2 in the $5^{12}6^4$ cages the spectrum shifts are close to half of those in aqueous solution.

Although we have tended to emphasise the fact that the halogens interact more weakly with the water in the hydrate cages than with liquid water, the halogen water interaction is crucial to the very existence of the solid hydrates. The halogen hydrates are among the most stable of such systems. Although BrCl hydrate has yet to be studied in detail, it could be the most stable of all [9]. In contrast to the Br_2 and I_2 shifts in their most stable hydrate cages, the shift for Cl_2 in the $5^{12}6^2$ cages is zero at 200 K and 500 cm^{-1} at 77K, while that of Br_2 in the $5^{12}6^4$ cages is only 360 cm^{-1}. The sensitivity to temperature of the Cl_2 hydrate spectrum emphasises how important it is to obtain similar data for the other halogens.

In some sense, the trend for the stretching vibrational frequencies in the hydrates is in contrast with the trends of the valence spectra. In aqueous solution the shift for Cl_2 is -22 cm^{-1}, from 560 down to 538 cm^{-1}. Again, the qualitative trend is as expected since

any halogen bonding is expected to weaken the Cl_2 bond. The calculated Cl_2 stretching frequency for the H_2O–Cl_2 dimer is only 530 cm^{-1} [60]. The higher vibrational frequency in aqueous solution compared to the free dimer is due to several effects, but again indicates that the halogen bond is not fully formed in aqueous solution. The Raman spectrum of Cl_2 in hydrate cages remains to be measured. For Br_2 the absolute change in the stretching frequency upon solvation is slightly smaller than for Cl_2: $-17\,cm^{-1}$ from 323 to 306 cm^{-1}. The bromine stretching frequency in the relatively 'tight' $5^{12}6^2$ cage is only slightly shifted from the gas phase, 321 cm^{-1}. The shift is somewhat less for the 'less tight' $5^{12}6^4$ cage, down to 317.5 cm^{-1}. Superficially, this is the opposite trend from what one might have expected from the valence spectra for which the larger cage appears to be relatively non-interacting. However, because the force between the guest atoms and the cage walls must be attractive, it is reasonable that a larger diameter cage will exert a net 'pull' on the two ends of the Br_2 bond. It would be very useful to obtain infrared intensities for these motions to see if the Br_2 is located asymmetrically in the larger cage. This would be quite a challenge. It is also interesting to note that the anharmonicity of the bromine stretching vibrations is lower in the hydrate cages than in the gas phase. This may have been expected if the bonds are slightly stretched at equilibrium, but the cage wall eliminates the possibility of dissociation. I_2 is expected to fit about as tightly in the $5^{12}6^4$ cage as Br_2 in the $5^{12}6^2$ cage, and, indeed, the stretching frequency in this case is unshifted from the gas phase. To our knowledge the iodine stretching frequency has not been measured in aqueous solution.

The ultrafast experiments of the Apkarian group provide more detailed time-dependent data to test future simulations. They also entice us with the prospect of measuring annealing of an amorphous environment into a hydrate in real time. As for the time-independent spectroscopy experiments, the results can be qualitatively described in terms of the several important interactions, but a quantitative simulation awaits future work. Apkarian suggests that the most useful approach to such simulations will involve factoring the important effects in a diatomics-in-molecule type model to better characterise the forces.

6. Overview of the theoretical studies

The insight theoretical tools provide that the nature of halogen–water interactions is crucial for achieving a molecular description of the macroscopic behaviour of halogens in aqueous environment. For this reason, a critical analysis of the proficiency of theoretical methods for predicting the structural and spectroscopic properties of halogens in water is needed. In this section we will summarise the studies of the last decade on the X–Y$\cdots$$H_2O$ systems and this will allow the analysis of the performance of the available *ab initio* and density functional theory (DFT) methods. These results are directly related to the gas phase studies, and we will also discuss the prospects for a deeper understanding of condensed phase phenomena.

6.1. *The interaction energies*

The reported interaction energies for the set of X–Y$\cdots$$H_2O$ complexes are given in Table 4. These values confirm that the interaction between water molecules and dihalogens ranges from weak to moderately strong. This trend can be understood using the simplest

Table 4. Comparison of the interaction energies in kcal mol^{-1} for the H_2O–X_2 and H_2O–X–Y complexes using *ab initio* and DFT methods.

Complex	DFT	Ref.	MP2	Ref.	CCSD(T)	Ref.
$F_2\cdots H_2O$	−1.26[a]	[80]	−0.67[b]	[80]	–	–
	−1.54[c]	[80]	−1.27[d]	[51]	–	–
$Cl_2\cdots H_2O$	−4.02[a]	[80]	−2.01[b]	[80]	−2.47[e]	[60]
	−2.91[c]	[80]	−2.82[f]	[52]	−2.62[g]	[60]
	–	–	−2.84[d]	[123]	−2.81[h]	[60]
	–	–	−2.85[i]	[137]	–	–
	–	–	−2.87[f]	*	–	–
	–	–	−2.82[j]	*	–	–
$Br_2\cdots H_2O$	−4.44[a]	[80]	−2.97[b]	[80]	−3.38[e]	[60]
	−3.72[c]	[80]	−3.65[d]	[123]	−3.48[g]	[60]
	−4.78[k]	[42]	−3.86[i]	[137]	−3.64[h]	[60]
	−4.06[l]	[42]	−4.30[m]	[42]	–	–
	–	–	−3.70[f]	*	–	–
	–	–	−3.62[j]	*	–	–
$I_2\cdots H_2O$	–	–	−4.57[n]	[137]	–	–
$ClF\cdots H_2O$	−6.58[a]	[80]	−4.43[b]	[80]	–	–
	−6.27[c]	[80]	−5.07[d]	[51]	–	–
	–	–	−5.12[o]	[93]	–	–
$BrF\cdots H_2O$	−7.59[a]	[80]	−6.35[b]	[80]	–	–
	−8.26[c]	[80]	−8.21[p]	[95]	–	–
$BrCl\cdots H_2O$	−5.89[a]	[80]	−3.62[b]	[80]	–	–
	−4.79[c]	[80]	−4.45[d]	[54]	–	–
	–	–	−4.35[p]	[94]	–	–

Note: *This work.
[a]B3LYP/6-31G*, BSSE corrected energies.
[b]MP2/6-311++G(d,p), BSSE corrected energies.
[c]B3LYP/6-311++G**, BSSE corrected energies.
[d]MP2/aug-cc-pVDZ, BSSE corrected energies.
[e]CCSD(T)/aVDZ, on MP2/aVTZ optimised geometries.
[f]MP2/aug-cc-pVDZ of counterpoise corrected optimised geometry.
[g]CCSD(T)/aVTZ, on MP2/aVTZ optimised geometries.
[h]CCSD(T)/aVQZ, on MP2/aVTZ optimised geometries.
[i]MP2/6-311++G(d,p).
[j]MP2/aug-cc-pVTZ of counterpoise corrected optimised geometry.
[k]B3LYP/6-31+G(d,p).
[l]B3LYP/6-311+G(d,p)
[m]MP2/6-311+G(d,p).
[n]MP2/6-311++G(d,p) and 6-311 for iodine.
[o]MP2(full)/aug-cc-pVTZ of counterpoise corrected optimised geometry.
[p]MP2/6-311++G(3d,3p) of counterpoise corrected optimised geometry.

electrostatic picture. The results are very sensitive to the size and presence of polarisation and diffuse functions on the basis set. Several authors [80,93,123] comment that even for triple-ξ quality basis sets, the basis set superposition error (BSSE) is not negligible and is of crucial importance for the systems containing bromine atoms. Accurate interaction energies for these complexes require a robust method for recovering the correlation effects

and, in that sense, coupled-cluster methods are the tools of choice. Several groups note that, for these types of interactions, MP2 level calculations overestimate the interaction energy roughly by 5% with respect to coupled-cluster methods [60,98,99]. Perhaps due to cancellation of errors [60], MP2 level calculations with a relatively small basis set, such as aVDZ, lead to results in reasonable agreement (± 0.01 kcal mol^{-1}) with CCSD(T) values.

The set of DFT results is not as large or varied as the *ab initio* results at least in part because it is known that DFT does not adequately represent the dispersion interaction. However, for many systems cancellation of errors results in stuctures and interaction energies in reasonable agreement with accurate *ab initio* calculations [99]. The B3LYP hybrid functional is most widely used due to its acceptable performance for describing hydrogen bonding. For the systems studied here, DFT methods show a consistent overestimation of the interaction energy. Karpfen [98] had convincingly showed that there are better alternatives functionals, e.g. BHHLYP, for halogen bonded systems. A word of caution on extrapolating the amines-halogen experience to these systems: all the Y–X$\cdots$NH$_3$ dimers are more strongly bound than the equivalent Y–X$\cdots$H$_2$O counterparts; 4.9 vs 2.8 kcal mol^{-1} for Cl_2; 6.9 vs 3.6 kcal mol^{-1} for Br_2; 14.6 vs 8.2 kcal mol^{-1} for BrF and 8.5 vs 4.3 kcal mol^{-1} for BrCl. This can be explained in terms of the stronger basicity of NH_3 but it might also be related to a higher electrostatic content in the interaction, thus explaining the reasonably good results using other functionals [82].

The experimental work suggests that the water–iodine interaction is especially interesting. However, iodine presents difficult problems for theory: balanced, large basis sets are not available and calibrated pseudo-potentials including relativistic effects have not been thoroughly tested. Work has started on the Rg–I_2 system [136] and Pathak *et al.* [137], have reported the interaction energy for H$_2$O$\cdots$I$_2$: -4.57 kcal mol^{-1}. Of course, these results from DFT need to be tested against *ab initio* calculations with correlation. Pseudo potentials for iodine have been tested or the Ar–I_2 dimer and have been found to be reasonably accurate [136]. It would be valuable to perform similar calculations for the H$_2$O$\cdots$I$_2$ dimer.

6.2. *The geometry of the complexes*

Table 5 reports the structural characteristics calculated for Y–X$\cdots$H$_2$O dimers. The typical signatures of this interaction are a lengthening of the X–Y bond and intermolecular distances shorter than the sum of the van der Waals radii [17]. These occur for all the complexes, and are present for all the *ab initio* levels of calculation [17]. The DFT methods often predict slightly shorter –X$\cdots$O distances than *ab initio* methods [123,137]. However, this is primarily when B3LYP is employed. The BHHLYP functional provides better results for Y–X$\cdots$H$_2$O dimers as it also does for X–Y$\cdots$NR systems [98].

For hydrogen bonded systems the BSSE error in the PES calculations has been analysed in detail. In particular, the intermolecular distance increases when the counterpoise correction is performed in the gradient optimisation. The observed changes depend on the level of theory and are larger if correlation energy is included at the MP2 level. In general, the results show that the weaker the interaction energy, the larger the effect of BSSE on the geometrical parameters, the vibrational frequencies, and on the binding energy [138]. This situation has been taken into account by Wu *et al.* [93–95], in their investigations of the interhalogen complexes. The counterpoise corrected optimisations for Cl_2 and Br_2 complexes with water that we report in this work, show that the

Table 5. Comparison of the experimentally derived structural parameters with values calculated using *ab initio* and DFT methodologies. Values are in Å.

	Experimental		DFT			MP2		
Complex	R(XY) [59]	R(–Y···O)	R(XY)	R(–Y···O)	Ref.	R(XY)	R(–Y···O)	Ref.
$F_2\cdots H_2O$	1.4119	2.748 [51]	–	2.387[a]	[80]	–	2.641[b]	[80]
	–	–	–	2.356[c]	[80]	1.432	2.600[d]	[51]
$Cl_2\cdots H_2O$	1.9878	2.8479 [52]		2.578[a]	[80]	–	2.780[b]	[80]
	–	–	–	2.667[c]	[80]	2.031	2.762[d]	[52]
	–	–	2.027	2.742[f]	[137]	–	2.755[d]	[123]
	–	–	2.066	2.712[g]	[137]	–	2.799[h]	[137]
	–	–	–	–	–	2.048	2.824[e]	*
	–	–	–	–	–	2.007	2.804[i]	*
$Br_2\cdots H_2O$	2.2811	2.8506 [53]	–	2.629[a]	[80]	–	2.823[b]	[80]
	–	–	–	2.733[c]	[80]	–	2.769[d]	[123]
	–	–	2.347	2.669[j]	[42]	2.324	2.791[d]	[53]
	–	–	2.352	2.740[k]	[42]	2.319	2.830[b]	[137]
	–	–	2.310	2.785[f]	[137]	2.318	2.826[l]	[42]
	–	–	2.345	2.762[g]	[137]	2.336	2.848[e]	*
	–	–	–	–		2.289	2.831[i]	*
$ClF\cdots H_2O$	1.6283	2.608(2) [51]	–	2.454[a]	[80]	–	2.588[b]	[80]
	–	–	–	2.457[c]	[80]	1.693	2.529[d]	[51]
	–	–	–			1.651	2.544[m]	[93]
$BrF\cdots H_2O$	1.7590	–	–	2.487[a]	[80]	–	2.572[b]	[80]
	–	–	–	2.501[c]	[80]	1.808	2.566[n]	[95]
$BrCl\cdots H_2O$	2.1361	2.7809(3) [54]	–	2.576[a]	[80]	–	2.765[b]	[80]
	–	–	–	2.655[c]	[80]	2.179	2.722[d]	[54]
	–	–	–	–	–	2.189	2.783[n]	[94]

Note: *This work
[a]B3LYP/6-31G*
[b]MP2/6-311++G(d,p)
[c]B3LYP/6-311++G**
[d]MP2/aug-cc-pVDZ
[e]MP2/aug-cc-pVDZ with counterpoise corrected gradient optimisation
[f]BHHLYP/6-311++G(d,p)
[g]B3LYP/6-311++G(d,p)
[h]MP2/6-311++G(d,p)
[i]MP2/aug-cc-pVTZ with counterpoise corrected gradient optimisation
[j]B3LYP/6-31+G(d,p)
[k]B3LYP/6-311+G(d,p)
[l]MP2/6-311+G(d,p)
[m]MP2(full)/aug-cc-pVTZ with counterpoise corrected gradient optimisation
[n]MP2/6-311++G(3d,3p) with counterpoise corrected gradient optimisation

correction on the energy of the minimum for bromine is larger than for chlorine (1.8:1) but the effect on the intermolecular distances is quite similar, 0.07 Å for chlorine and 0.06 Å for bromine. In each case, the corrected geometries are in much better agreement with the experimentally derived values.

Considerably less attention has been focused on the other stable conformers of the $Y–X\cdots H_2O$ dimers. Ramondo *et al.* [42], were the first to describe the H-bonded structure

for bromine. Their calculations showed that this isomer was considerably more weakly bonded than the X-bonded structure: *ab initio* methods predicted it to be 20% as strong and DFT 11%. Hydrogen bonded structures were also described for all the interhalogen compounds [93–95]. In those complexes the halogen atom that binds to the water molecule is the more electronegative of the pair, e.g. Cl–F···HOH: an important difference from the corresponding halogen bond geometry. The stability difference between the two possible isomers is again large, the halogen bond energy is 3.9–4.5 times more than the hydrogen bond energy. As we have recently reported, this type of coordination between water and dihalogens is weaker than hydrogen bonding due to its large dispersion content. Thus they have more in common with van der Waals bonds than strong hydrogen bonds. Interestingly, even though the interaction is relatively weak, $E_{int} < 2.0\,kcal\,mol^{-1}$, the intermolecular distances are still considerably smaller than the sum of the van der Waals radii: 2.6 and 2.7 Å for the Cl_2 and Br_2 structures, 2.2 Å for F and 2.8 Å for Cl in the complexes of the interhalogen complexes. However, the perturbations of the properties of the dihalogens constituent for these isomers are not as large as the ones produced by either the hydrogen or halogen bonds. This will be discussed below.

6.3. *Spectroscopical properties*

The microwave, infrared and UV-vis spectra of the halogens have been very useful for studying the role of intermolecular forces in various environments, and have provided important results for testing theory as it becomes ever more powerful for calculating the properties of clusters and condensed phase systems. The formation of halogen bonds is expected to be accompanied by red shifts of the stretching frequencies of the dihalogen due to the redistribution of the charge density. Alkorta *et al.* [80], were the first group that systematically analysed those changes and their results are in excellent agreement with more recent calculations [93–95,123]. The X–Y harmonic stretching frequencies for the X–Y···H_2O complexes shift by 10–30 cm^{-1}, with the homonuclear dihalogens, (25–10 cm^{-1} from F_2 to Br_2) being less perturbed than for the interhalogen compounds (30–12 cm^{-1} from FCl to ClBr). The larger the size of the dihalogen molecule the smaller the calculated shift. So far, there is little experimental data regarding these trends, resonance Raman spectroscopy may be a useful tool for such studies in the near future.

In contrast to calculations of vibrational frequencies, calculations on the excited states of the halogen bound complexes have only recently been performed. Hernández-Lamoneda *et al.* [60], produced highly refined 2D PES to investigate the coupling of the inter- (–X···O) and the intramolecular (X–Y) interactions. The transition moments also show a high correlation with the degrees of freedom investigated. The vertical electronic transitions from the ground state to the lowest of the $^1\pi$ states of Cl_2 and Br_2 in the 1:1 complexes with water were calculated and found to be blue shifted with respect to the free halogen molecule: ~1600 cm^{-1} for Cl_2 and ~2000 cm^{-1} for Br_2. These blue-shifts are considerably larger than those measured in condensed phases. To explain this difference the inclusion of several other solvent molecules as well as a more sophisticated simulation of the spectra will be required.

A recent paper has reported several refinements to the study discussed in the previous paragraph for the H_2O···Cl_2 dimer. The 2D PES of H_2O···Cl_2, were corrected by the

explicit consideration of spin–orbit coupling. An explicit calculation of the ground state nuclear wavefunction and a wavepacket analysis of the excited state dynamics were used to calculate the valence electronic absorption spectrum within the 2D model [139]. The improved calculated value of the dimer blue-shift is $1250\,cm^{-1}$ compared to the previous values for vertical excitation, $1600\,cm^{-1}$. The largest contribution to this difference is the zero point energy of the ground state. A second effect is that the slightly longer Cl–Cl distance in the dimer results in Franck–Condon excitation to a less repulsive part of the **C** state potential. A surprising result of the 2D spectrum calculation for $H_2O\cdots Cl_2$ calculation is that it is slightly *narrower* than that of the free Cl_2 molecules. This is due to subtle changes in the Cl–Cl potential in the ground and excited states. It will be very valuable to include more of the intermolecular coordinates and to extend these calculations to larger clusters, especially ones that are likely to mimic the local environment in aqueous solution.

6.4. *Adding solvent molecules*

One of the goals in the work reported here is to provide more insight into complex condensed phase phenomena. In this sense, the detailed study of the smallest 1:1 complexes has provided a much better understanding of the nature of the interactions that are relevant for the solvation process. In the route to hydration, assessing the size of the collective effects is an important step for providing a more detailed and accurate description of solubility differences, reactivity in aqueous media and modulation of spectroscopic properties by the environment of a molecule. These three issues have provided a focus for recent theoretical work on halogen–water clusters. In the study of bromine on ice surfaces [42] theoretical calculations on small Br_2–water clusters with up to seven water molecules identified an enhancement of the polarisation of the dihalogen as a consequence of simultaneous X-bonding and XH-bonding that is accompanied by a lengthening of the Br–Br bond that eventually leads to its ionic dissociation. The bond dissociation process as a consequence of collective effects has also been identified for other molecules and for water itself [140].

Pathak *et al.* [137] studied the change of the polarisabilities of the clusters as a possible explanation of the differences in solubility of gaseous Cl_2, Br_2 and I_2 in liquid water. Their work found that the stable structures of the clusters for the three species are quite similar and concluded that due to the large polarisation effects, Br_2 and I_2 can be considered as a charge separated ion pair in the clusters. The larger stability of the clusters containing iodine compared to chlorine led them to suggest that the solubility of I_2 is larger than that of chlorine. However, the stability of the cluster is not a direct measure of the free energy of hydration of the dihalogen molecules in liquid water. Iodine is less soluble then either Cl_2 or Br_2 [27] indicating that the nearest neighbour attractive forces do not dominate this property. Solvation of the halogen molecules is intermediate between that of hydrogen bonding and non-interactive solutes and, for that reason, the hydrophobic component of solvation, the entropic effects, must be carefully considered [141].

Motivated by the large blue shifts calculated for the halogen bound 1:1 clusters of Cl_2 and Br_2, we have recently studied the structure of clusters with Cl_2 or Br_2 with up to five water molecules. Several stable structures were identified for each size and it was possible to assess the role that collective effects have on the spectroscopic properties. It is convenient to classify three different forces involved in the stability and behaviour of

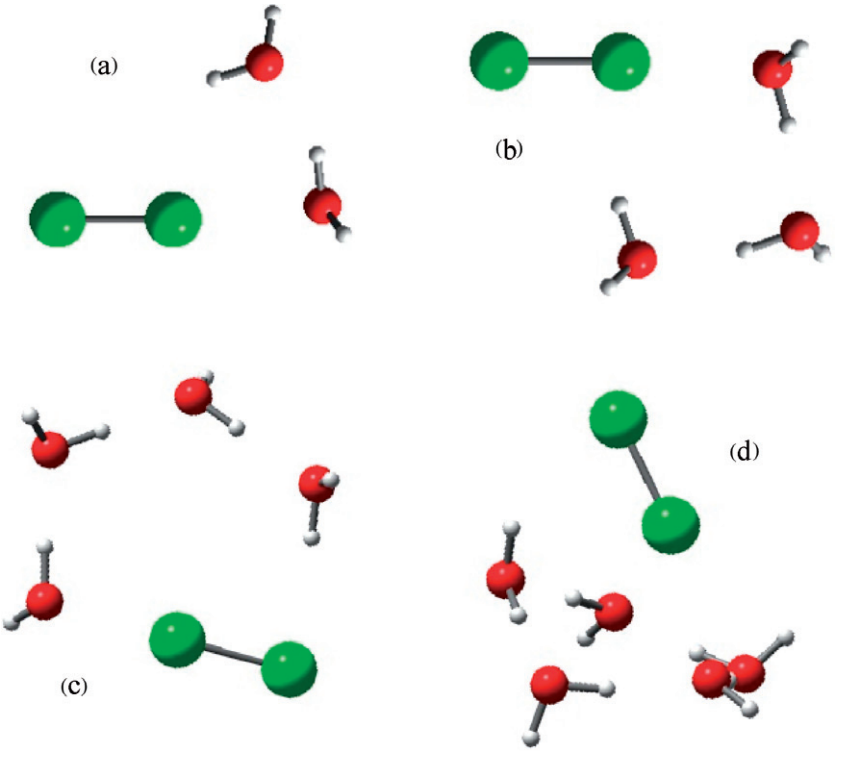

Figure 12. [Colour online] Selected stable structures for the $Cl_2\cdots(H_2O)_n$ clusters for which the three, HB, XB and XH, prevalent types of molecular interactions are present.

these clusters: the hydrogen bonds between water molecules (HB), the halogen bonds between water and the halogens (XB) and the hydrogen–halogen bonds between water and halogens (XH). As discussed above, the latter case is dominated by dispersion and is not a true example of hydrogen bonding. A representative sample of the stable structures found is shown in Figure 12. Because HB is the strongest intermolecular force in these systems, optimisation of the water–water interaction is favoured over the water–halogen interactions. However, the many body analysis confirmed that HB are enhanced by the presence of XB in the cluster. XB have strong effects on the vibrational and electronic spectroscopic properties, whereas XH interactions have little effect on the vibrational spectra and only yield a moderate blue shift of the valence electronic spectrum, $\sim 500\,cm^{-1}$. As for the previously studied dimers, the calculated blue shifts for these larger clusters are still more than those observed in aqueous solution. There is no apparent trend in the shifts and it is clear that much more work will be required to reach even a qualitative interpretation of condensed phase spectra.

Shofield and Jordan [142] recently studied the electronic transitions of Cl_2 in 5^{12} and $5^{12}6^2$ water cages, the two building units of chlorine hydrate-clathrate. Due to the size of the system and the symmetry restrictions that are required for making feasible and meaningful calculations, this is currently the upper limit of *ab initio* cluster calculations, especially for the excited states. The time involved for such calculations did not allow them

to consider geometries other than those with Cl_2 at the centre of the cages, so they did not map out the potential for the Cl_2 in the cage. Using an approximate coupled-cluster method (RICC2) they calculated the blue shift of valence electronic spectrum to be small. They also calculated that UV transitions resulting from electron transfer from the Cl_2 to the water cage will be strongly shifted to lower energy.

For several organic molecules, the solvatochromic effects can be well described using refined continuum models [34,143]. For the halogens, it will probably be necessary to describe specific nearest neighbour interactions in addition to perturbation of the chromophore by the environment. It may be useful to employ models in which the description of the halogen chromophore includes specific nearest neighbour interaction and then the superchomophore is embedded in a bulk solvent. The gas phase results may be useful for testing the assumptions in the superchromophore part of these calculations. Preliminary calculations on the effect of the dielectric constant on the vertical transitions of chlorine show that the bulk dielectric of solvent shift red shift is $\sim 550\,cm^{-1}$ [139]. Recent progress on different solvent models yields interesting results for the solvation free energy [34,144]; however, it remains to be seen if these results can be generalised to a wide variety of solvents, solutes and properties of the resulting solvation [143,145].

One reason the halogen hydrates are so interesting is that their stability depends on the full range of intermolecular forces, from dispersion to chemical bonding. The success attained for smaller systems in 'building solutions one molecule at a time' [146] is not an approach possible for this system since *ab initio* calculations for even the smaller solvated units are difficult to converge, and still not reflective of bulk properties. As for many solvation phenomena, it is expected that numerical simulations with modern empirical model potentials may provide insight into the complexity of hydrates. Shofield and Jordan [147] have developed a polarisable force field for application to the bromine hydrates, and they have applied it to the difficult problem of which of the bromine hydrate structures is the most stable. They constructed CS-I, CS-II and TS-I hydrate lattices on the computer and put bromine molecules in each of the $5^{12}6^2$, $5^{12}6^3$ and $5^{12}6^4$ cages, leaving the 5^{12} cages empty. They performed molecular dynamics simulations with rigid H_2O and Br_2 molecules from 80 to 260 K and calculated the time average of the energy for each crystal structure and temperature. This data was then used to evaluate the stability of each crystal structure based on the average energy, which is in the decreasing order: CS-II > CS-I > TS-I. The range of differences is only $0.1\,kcal\,mole^{-1}$ H_2O. So, it is perhaps not too surprising that we were able to observe all three structures. Entropy probably plays an important role in deciding which structure is the most stable at a given temperature and composition.

Comparing crystal structure stabilities is complicated by the fact that the three crystals have different $H_2O:Br_2$ stoichiometries: assuming perfect cage filling, CS-I = 7.67, TS-I = 8.6 and CS-II = 17. Schofield and Jordan used the value 7.67, which favours the CS-I crystal. To partially compensate, they allowed the excess bromine to form solid bromine, lowering the energy disadvantage for the other two structures. Note that all of the bromine in the CS-I structure is in $5^{12}6^2$ cages, while in the TS-I structure 80% is in $5^{12}6^2$ cages, 20% in $5^{12}6^3$ cages. Since the TS-I crystal is more stable than CS-I the $5^{12}6^3$ cages are particularly well suited for storing bromine. Schofield and Jordan calculate the energy difference for adding bromine to $5^{12}6^2$ and $5^{12}6^3$ cages to be 1 kcal per (mole of cages). This is probably an underestimate, since their potential appears to underestimate

the repulsion between bromine and the cage walls, leading to an overestimation of the stability of bromine in $5^{12}6^2$ cages.

Another interesting difference between the three hydrate structures is the inherent stability of the lattices before the bromine is added. Pentagonal faces strain the hydrogen bond bend less than hexagonal faces, so one expects the structure with more of the water molecules in 5^{12} cage faces to be the more stable. In this regard, the CS-II structure has an advantage since it has the highest fraction of 5^{12} cages. The Schofield and Jordan molecular dynamics study estimates this advantage to be about 0.05 kcal mole^{-1} (H_2O) for CS-II relative to TS-I and 0.07 kcal mole^{-1} (H_2O) for CS-II relative to CS-I. The advantage of CS-II over TS-I and CS-I increases with temperature. This may play an important role in determining which structure is more stable at a given temperature. For the empty lattices, Schofield and Jordan calculated that entropy favours CS-I at all temperatures, but the differences were small compared to the potential energy. It is clear that the relative stabilities of the three bromine hydrate lattices are not very different, and that a quantitative evaluation of stability will require quite accurate calculations.

In their pioneering crystal structure of chlorine hydrate, Pauling and Marsh used van der Waals radii to justify assuming that there were no chlorine molecules in the 5^{12} cages. Cady later showed that this assumption is incorrect. If Cl_2 is placed in the experimentally determined 5^{12} cage structure with the ends pointing toward the middle of opposing pentagonal faces to obtain the largest possible Cl$\cdots$O nearest neighbour distance, the value is 3.11 Å, 0.16 Å shorter than the sum of the van der Waals radii. If the Cl_2 is instead aligned between two of the cage wall oxygen atoms, the Cl$\cdots$O distance is 2.94 Å, significantly shorter. While this is somewhat longer than the optimised Cl$\cdots$O distance for a $H_2O\cdots Cl_2$ halogen bonded dimer, it is probably an unfavourably short difference for this configuration. In their *ab initio* calculation of the orientation of Cl_2 in the 5^{12} cage, Jordan and Schofield allowed the cage to distort from the X-ray coordinates with the Cl_2 aligned between oxygen atoms. Even with the 5^{12} cage being allowed to distort, the energy for adding Cl_2 was only 2.3 kcal mole^{-1}, relative to the equally distorted, but unoccupied, cage. To date, there is no estimate for the energy of adding Cl_2 to the $5^{12}6^2$ cages. In this case, if the Cl_2 aligns between two of the oxygen atoms on opposing sides of the cage, the Cl$\cdots$O nearest neighbour distance is 3.6 Å, somewhat greater than the sum of the Cl and O van der Walls radii. Given that the dissociation temperature of chlorine hydrate is 283 K, 5 K higher than that of bromine hydrate, one may expect this stabilisation to be substantial.

Finally, we make a brief comment on the lack of a stable structure for pure iodine hydrate clathrate. Given that Br_2 in the $5^{12}6^2$ cage is quite stable, and that the diameter of the $5^{12}6^4$ cage is 0.9 Å greater than the long axis of the $5^{12}6^2$ cage, and that the van der Waals 'length' of I_2 is expected to be $\sim$0.7 Å longer than that of Br_2, it seems likely that the CS-II iodine clathrate hydrate structure should be close to the stability zone. This hypothesis is supported by our finding that small amounts of I_2 readily substitute for the very stable THF in $5^{12}6^4$ cages. It may be possible to create a double clathrate with another guest in the small cages and I_2 in the large cages.

In this section we have reviewed a very large body of theoretical work on the interactions of halogen molecules with water, and compared this work to several similar problems, especially hydrogen bonding. It is clear that much progress has been made. The energies and spectroscopic properties of the ground electronic states of moderate sized clusters can now be calculated with confidence, and the roles of the various intermolecular

forces can be described in some detail. Experiments to test these calculations for larger clusters would be very valuable. Even for electronic excited states recent progress is quite promising, and, again, comparisons with experiments will be very important. The frontier for the type of work described here is to incorporate our detailed knowledge regarding small clusters into useful models for condensed phase systems. Aqueous solvation and halogen hydrates provide particularly challenging problems in this regard.

7. Summary and prospects for further understanding

Since the initial discovery of the halogens, their chemistry has been closely linked to that of water. Halogen hydrates were discovered at the beginning of the 19th century, and the spectroscopy of halogen molecules in aqueous solution was being studied by the end of that century. For the first half of the 20th century serious attempts to achieve a microscopic understanding of these spectra were being made. The matrix isolation and supersonic expansion techniques made it possible to study individual dimers, and this led to much deeper understanding of the intermolecular force and the naming of 'halogen bonds'. Halogen bonds are one step down from hydrogen bonds in bond strength, but still much stronger than typical electrostatic and van der Waals bonding in other systems. In $H_2O\cdots X_2$ dimers, halogen bonding has its full effect and the calculated effects on both electronic and vibrational spectra are even larger than for aqueous solution. In large clusters and solution, hydrogen bonding takes precedence and the effects of halogen bonding are smaller. Clathrate hydrates present an intermediate case between van der Waals and halogen bonding. The halogen molecule guests in the clathrate hydrate cavities are not able to achieve their preferred orientation with the water molecules in the cage walls since these water molecules are even more completely hydrogen bonding that those in aqueous solution.

We propose that theoretical methods are just now becoming powerful enough to attack the analysis of water–halogen interactions in larger clusters, aqueous solution and clatharate hydrates. We have been pursuing *ab initio* methods to study the building block for these complicated systems. It is clear that, for the near future, more efficient methods must be employed for the bulk properties. Some possible approaches are: (1) hybrid methodologies, i.e. *ab initio*, including more refined DFT methods for describing the first solvation shell and embedding this in a continuum model for the bulk; (2) semi-empirical force field models that have been parameterised to reproduce high quality *ab initio* PES for model problems; (3) empirical models such as extensions of the one recently proposed by Schofield and Jordan; (4) diatomics-in-molecule approaches as proposed by Apkarian. Each of these methods has advantages and disadvantages, and further progress will probably involve insights gained from each of the techniques.

We believe that the work reviewed here already makes the water–halogen system one of the best characterised solvent–solute systems from an experimental point of view. Having data for both liquid and solid solutions provides a rich context for further theoretical refinements. However, there is still much work for the experimentalists. Among the paths that appear to hold out promise are: (1) spectroscopic studies of larger clusters to investigate molecule by molecule solvation; (2) measuring the temperature dependence of the hydrate spectra to search for signs of localisation of the halogens within the cages; (3) complimenting the spectroscopic studies with temperature dependent X-ray diffraction work; (4) thermodynamic measurements of hydrate stability. So far, we have focused

on spectroscopy, structure and stability. The kinetics of hydrate formation, dissociation and interconversion of crystal structures is also of great interest. The Apkarian group is pursuing Raman studies that should shed light on these processes.

We expect that understanding the water–halogen interactions will continue to be a focus at the frontier of chemical physics for some time to come.

Acknowledgements

We are very grateful to our colleagues: Everly Fleischer, V. Ara Apkarian, Ilya Goldshleger, Jordan Pio, Molly Taylor, Edward Branigan, Megan Johnson, Joanne Abbonbondola, Melissa Prado, Kenneth Jordan, Daniel Schofield, Ramón Hernández-Lamoneda, Oscar I. Arillo, Nadine Halberstadt and Tahra Ayed for many valuable inputs to the work discussed here. The Irvine work was supported by the United States National Science Foundation grant No. CHE-0404743. M.I. Bernal-Uruchurtu acknowledges the financial support of UC-MEXUS/CONACYT for her sabbatical year fellowship.

References

[1] H. Davy, Philos. Trans. R. Soc. London **101**, 155 (1811).
[2] L. Pauling and R. E. Marsh, Proc. Nat. Acad. Sci. **38**, 112 (1952).
[3] K. Udachin, C. I. Ratcliffe, and J. A. Ripmesteer, J. Supramolecular Chem. **2**, 405 (2002).
[4] E. Beckmann, Z. Phyzik. Chem. **5**, 76 (1889).
[5] C. Gautier and M. Charpy, Compt. Rend. **110**, 645 (1890).
[6] D. G. Jahn, W. S. Barney, J. Cabalo, S. G. Clement, and N. Halberstadt, J. Chem. Phys. **104**, 3501 (1996).
[7] J. M. Pio, W. E. van der Veer, C. R. Bieler, and K. C. Janda, J. Chem. Phys. **128**, 134311 (2008).
[8] D. S. Boucher, D. B. Strasfeld, R. A. Loomis, J. M. Herbert, S. E. Ray, and A. B. McCoy, J. Chem. Phys. **123**, 104312 (2005).
[9] D. N. Glew and D. A. Hames, Can. J. Chem. **47**, 4651 (1969).
[10] L. J. Gay-Lussac and L. J. Thénard, Mémoires de Physique et de Chimie de la Société d'Arcueil **2**, 339 (1809).
[11] H. Davy, Philos. Trans. R. Soc. London **108**, 169 (1818).
[12] M. Faraday and H. Davy, Phil. Trans. R. Soc. London **113**, 160 (1823).
[13] M. Faraday, Q. J. Sci. **15**, 71 (1823).
[14] M. v. Stackelberg, O. Gotzen, J. Pietuchovsky, O. Witscher, H. Fruhbuss, and W. Meinhold, Fortschr. Mineral. **26**, 122 (1947).
[15] W. F. Claussen, J. Chem. Phys. **19**, 259 (1951).
[16] W. F. Claussen, J. Chem. Phys. **19**, 1425 (1951).
[17] A. Bondi, J. Phys. Chem. **68**, 441 (1964).
[18] J. H. van der Waals and J. C. Platteeuw, Adv. Chem. Phys. **2**, 1 (1959).
[19] G. H. Cady, J. Phys. Chem. **87**, 4437 (1983).
[20] K. W. Allen and G. A. Jeffrey, J. Chem. Phys. **38**, 2304 (1963).
[21] Y. A. Dyadin and V. R. Belosludov, in *Comprehensive Supramolecular Chemistry*, edited by J. L. Atwood, J. E. D. Davies, D. D. Malnicol, and F. Vogtle (Pergamon, New York, 1996), Vol. 6, p. 79.
[22] Y. A. Dyadin and L. S. Aladko, Zh. Struct. Khim. **18**, 51 (1977).
[23] K. A. Udachin, G. D. Enright, C. I. Ratcliffe, and J. A. Ripmeester, J. Am. Chem. Soc. **119**, 11481 (1997).

[24] G. Kerenskaya, I. U. Goldschleger, V. A. Apkarian, and K. C. Janda, J. Phys. Chem. A **110**, 13792 (2006).
[25] I. U. Goldschleger, G. Kerenskaya, K. C. Janda, and V. A. Apkarian, J. Phys. Chem. A **112**, 787 (2008).
[26] G. Kerenskaya, I. U. Goldschleger, V. A. Apkarian, E. Fleischer, and K. C. Janda, J. Phys. Chem. A **111**, 10969 (2007).
[27] F. A. Cotton and G. Wilkinson, *Advanced Inorganic Chemistry*, 3rd ed. (Wiley, New York, 1972).
[28] J. H. Hildebrand and B. L. Glascock, J. Am. Chem. Soc. **31**, 26 (1909).
[29] R. S. Mulliken, J. Am. Chem. Soc. **72**, 600 (1950).
[30] N. S. Bayliss, Nature **163**, 764 (1949).
[31] R. S. Mulliken, J. Phys. Chem. **56**, 801 (1952).
[32] J. Ham, J. Am. Chem. Soc. **76**, 3886 (1954).
[33] R. I. Gray, K. M. Luckett, and J. Tellinghuisen, J. Phys. Chem. A **105**, 11183 (2001).
[34] R. Cammi, S. Corni, B. Mennucci, and J. Tomasi, J. Chem. Phys. **122**, 104513 (2005).
[35] O. Hassel and C. Romming, Q. Rev. (London) **16**, 1 (1962).
[36] L. Fredin and B. Nelander, J. Mol. Struct. **16**, 217 (1973).
[37] A. Engdahl and B. Nelander, J. Chem. Phys. **84**, 1981 (1986).
[38] A. Engdahl and B. Nelander, Chem. Phys. **100**, 273 (1985).
[39] P. N. Noble and G. C. Pimentel, Spectrochim. Acta, Part A **24**, 797 (1968).
[40] T. C. McInnis and L. Andrews, J. Phys. Chem. **96**, 2051 (1992).
[41] K. Johnsson, A. Engdahl, P. Ouis, and B. Nelander, J. Phys. Chem. **96**, 5778 (1992).
[42] F. Ramondo, J. R. Sodeau, T. B. Roddis, and N. A. Williams, Phys. Chem. Chem. Phys. **2**, 2309 (2000).
[43] S. E. Nowick, K. C. Janda, and W. Klemperer, J. Chem. Phys. **65**, 5115 (1976).
[44] A. C. Legon, in *Halogen Bonding: Fundamentals and Applications*, edited by P. Metrangolo and G. Resnati (Springer, Berlin, 2008), Vol. 126, pp. 17–64.
[45] A. C. Legon and D. J. Millen, Chem. Soc. Rev. **16**, 467 (1987).
[46] A. C. Legon, Chem. Eur. J. **4**, 1890 (1998).
[47] W. T. Pennington, T. W. Hanks, and H. D. Arman, in *Halogen Bonding: Fundamentals and Applications*, edited by P. Metrangolo and G. Resnati (Springer, Berlin, 2008), Vol. 126, pp. 65–104.
[48] P. Metrangolo, H. Neukirch, T. Pilati, and G. Resnati, Acc. Chem. Res. **38**, 386 (2005).
[49] P. Metrangolo and G. Resnati, Science **321**, 918 (2008).
[50] S. A. Cooke, G. Cotti, J. H. Holloway, and A. C. Legon, Angew. Chem. Int. Ed. **36**, 129 (1997).
[51] S. A. Cooke, G. Cotti, C. M. Evans, J. H. Holloway, Z. Kisiel, A. C. Legon, and J. M. A. Thumwood, Chem. Eur. J. **7**, 2295 (2001).
[52] J. B. Davey, A. C. Legon, and J. M. A. Thumwood, J. Chem. Phys. **114**, 6190 (2001).
[53] A. C. Legon, J. M. A. Thumwood, and E. R. Waclawik, Chem. Eur. J. **8**, 940 (2002).
[54] J. B. Davey and A. C. Legon, Phys. Chem. Chem. Phys. **3**, 3006 (2001).
[55] J. B. Davey, A. C. Legon, and E. R. Waclawik, Phys. Chem. Chem. Phys. **2**, 1659 (2000).
[56] Z. Kisiel, A. C. Legon, and D. J. Millen, Proc. R. Soc London Series A – Math. Phys. Eng. Sci. **381**, 419 (1982).
[57] A. C. Legon and L. C. Willoughby, Chem. Phys. Lett. **95**, 449 (1983).
[58] S. A. Cooke, G. Cotti, C. M. Evans, J. H. Holloway, and A. C. Legon, Chem. Comm. **20**, 2327 (1996).
[59] *CRC handbook of chemistry and physics*, 89th Edition (Internet Version 2009) ed. (CRC Press/ Taylor & Francis, Boca Raton, Fl., 2009).
[60] R. Hernández-Lamoneda, V. H. Uc-Rosas, M. I. Bernal-Uruchurtu, N. Halberstadt, and K. C. Janda, J. Phys. Chem. A **112**, 89 (2008).
[61] N. G. Lewis, J. Franklin Inst. **226**, 293 (1938).

[62] N. V. Sidgwick, *The Electronic Theory of Valency* (Oxford University Press, Oxford, 1929).
[63] O. Hassel, Proc. Chem. Soc. London **9**, 250 (1957).
[64] O. Hassel and K. O. Stromme, Nature **182**, 1155 (1958).
[65] T. Bjorvatten, C. Romming, and O. Hassel, Nature **189**, 137 (1961).
[66] P. Groth and O. Hassel, Proc. Chem. Soc. London, **September**, 379 (1962).
[67] O. Hassel, *Structural aspects of interatomic charge-transfer bonding*, Nobel lecture, 9 June 1970.
[68] G. Leroy and G. Louterman-Leloup, J. Mol. Struct. **28**, 33 (1975).
[69] M. J. S. Dewar and C. C. J. Thompson, Tetrahedron **S7**, 97 (1966).
[70] J. P. Malrieu and P. Claverie, J. Chim. Phys. **65**, 735 (1968).
[71] T. Dahl and I. Roeggen, J. Am. Chem. Soc. **118**, 4152 (1996).
[72] P. Metrangolo and G. Resnati, Chem. Eur. J. **7**, 2511 (2001).
[73] P. Metrangolo, F. Meyer, T. Pilati, G. Resnati, and G. Terraneo, Angew. Chem. Int. Ed. **47**, 6114 (2008).
[74] T. Clark, M. Hennemann, J. Murray, and P. Politzer, J. Mol. Model. **13**, 291 (2007).
[75] P. Politzer, P. Lane, M. Concha, Y. Ma, and J. Murray, J. Mol. Model. **13**, 305 (2007).
[76] A. Rohrbacher, J. Williams, and K. C. Janda, Phys. Chem. Chem. Phys. **1**, 5263 (1999).
[77] K. Higgins, F. M. Tao, and W. Klemperer, J. Chem. Phys. **109**, 3048 (1998).
[78] A. A. Buchachenko, T. Gonzalez-Lezana, M. I. Hernández, M. P. D. Castells, G. Delgado-Barrio, and P. Villarreal, Chem. Phys. Lett. **318**, 578 (2000).
[79] R. Hernández-Lamoneda and K. C. Janda, J. Chem. Phys. **123**, 161102 (2005).
[80] I. Alkorta, I. Rozas, and J. Elguero, J. Phys. Chem. A **102**, 9278 (1998).
[81] O. K. Poleshchuk and A. C. Legon, Zeitschrift Fur Naturforschung Sec. A – J. Phys. Sci. **57**, 537 (2002).
[82] A. Karpfen, Theor. Chem. Acc. **110**, 1 (2003).
[83] C. Ouvrard, J.-Y. Le Questel, M. Berthelot, and C. Laurence, Acta Crystal. Sec. B **59**, 512 (2003).
[84] W. Wang, N.-B. Wong, W. Zheng, and A. Tian, J. Phys. Chem. A **108**, 1799 (2004).
[85] J.-W. Zou, Y.-J. Jiang, M. Guo, G.-X. Hu, B. Zhang, H.-C. Liu, and Q.-S. Yu, Chem. Eur. J. **11**, 740 (2005).
[86] Y. X. Lu, J. W. Zou, Y. H. Wang, and Q. S. Yu, J. Mol. Struct. Theochem **776**, 83 (2006).
[87] Y.-X. Lu, J.-W. Zou, Y.-H. Wang, and Q.-S. Yu, J. Mol. Struct. Theochem **767**, 139 (2006).
[88] Y.-X. Lu, J.-W. Zou, Q.-S. Yu, Y.-J. Jiang, and W.-N. Zhao, Chem. Phys. Lett. **449**, 6 (2007).
[89] J. S. Murray, P. Lane, and P. Politzer, Int. J. Quantum Chem. **107**, 2286 (2007).
[90] P. Politzer, J. S. Murray, and P. Lane, Int. J. Quantum Chem. **107**, 3046 (2007).
[91] K. E. Riley and K. M. Merz, J. Phys. Chem. A **111**, 1688 (2007).
[92] F. F. Wang, J. H. Hou, Z. R. Li, D. Wu, Y. Li, Z. Y. Lu, and W. L. Cao, J. Chem. Phys. **126**, 144301 (2007).
[93] J. Wu, J. Zhang, Z. Wang, and W. Cao, J. Chem. Theor. Comput. **3**, 95 (2007).
[94] J. Wu, J. Zhang, Z. Wang, and W. Cao, Int. J. Quantum Chem. **107**, 1897 (2007).
[95] J. Y. Wu, J. C. Zhang, Z. X. Wang, and W. L. Cao, Chem. Phys. **338**, 69 (2007).
[96] J. S. Murray, M. C. Concha, P. Lane, P. Hobza, and P. Politzer, J. Mol. Model. **14**, 699 (2008).
[97] W. Wang and P. Hobza, J. Phys. Chem. A **112**, 4114 (2008).
[98] A. Karpfen, in *Halogen Bonding: Fundamentals and Applications*, edited by P. Metrangolo and G. Resnati (Springer-Verlag, Berlin, 2008), Vol. 126, p. 1.
[99] K. E. Riley and P. Hobza, J. Chem. Theor. Comput. **4**, 232 (2008).
[100] Z. D. L. Zhi-Ru, L. Ze-Sheng, H. Hu-Ri, F.-M. Tao, and S. Chia-Chung, J. Phys. Chem. A **105**, 1163 (2001).
[101] W. H. Thomson and J. T. Hynes, J. Am. Chem. Soc. **122**, 6278 (2000).
[102] L. Rincon, R. Almeida, D. García-Aldea, and H. Diez y Riega, J. Chem. Phys. **114**, 5552 (2001).
[103] C. Chipot, L. Gorb, and J. L. Rivail, J. Phys. Chem. **98**, 1601 (1994).

[104] C. Lee, C. Sosa, M. Planas, and J. J. Novoa, J. Chem. Phys. **104**, 8 (1996).
[105] K. A. Tay and F. Bresme, Phys. Chem. Chem. Phys. **11**, 409 (2009).
[106] D. E. Bacelo, J. Phys. Chem. A **106**, 11190 (2002).
[107] A. Milet, C. Struniewicz, R. Moszynski, and P. E. S. Wormer, J. Chem. Phys. **115**, 349 (2001).
[108] N. Uras-Aytemiz, C. Joyce, and J. P. Devlin, J. Phys. Chem. A **105**, 10497 (2001).
[109] G. M. Chaban, R. B. Gerber, and K. C. Janda, J. Phys. Chem. A **105**, 8323 (2001).
[110] Y. A. Mantz, F. M. Geiger, L. T. Molina, M. J. Molina, and B. L. Trout, J. Phys. Chem. A **105**, 7037 (2001).
[111] E. Cabaleiro-Lago, J. M. Hermida-Ramón, and J. Rodríguez-Otero, J. Chem. Phys. **117**, 3160 (2002).
[112] A. Al-Halabi, R. Bianco, and J. T. Hynes, J. Phys. Chem. A **106**, 7639 (2002).
[113] N. Dozova, L. Krim, M. E. Alikhani, and N. Lacome, J. Phys. Chem. A **111**, 10055 (2007).
[114] S. Odde, B. J. Mhin, S. Lee, H. M. Lee, and K. S. Kim, J. Chem. Phys. **120**, 9525 (2004).
[115] A. Goursot, G. Fischer, C. C. Lovallo, and D. R. Salahub, Theor. Chem. Acc. **114**, 115 (2005).
[116] S. Odde, B. J. Mhin, K. H. Lee, H. M. Lee, P. Tarakeshwar, and K. S. Kim, J. Phys. Chem. A **110**, 7918 (2006).
[117] M. Masia, H. Forbert, and D. Marx, J. Phys. Chem. A **111**, 12181 (2007).
[118] O. I. Arillo-Flores, M. F. Ruiz-López, and M. I. Bernal-Uruchurtu, Theor. Chem. Acc. **118**, 425 (2007).
[119] K. Morokuma, J. Chem. Phys. **55**, 1236 (1977).
[120] A. R. Reed, L. A. Curtiss, and F. Weinhold, Chem. Rev. **88**, 899 (1988).
[121] B. Jeziorski, R. Moszinsky, and K. Szalewicz, Chem. Rev. **94**, 1887 (1994).
[122] A. Martín Pendás, M. A. Blanco, and E. Francisco, J. Chem. Phys. **125**, 184112 (2006).
[123] M. I. Bernal-Uruchurtu, R. Hernández-Lamoneda, and K. C. Janda, J. Phys. Chem. A **113**, 5496 (2009).
[124] X. Y. Zhang, L. P. Meng, Y. L. Zeng, Y. Zhao, and S. J. Zheng, Acta Chimica Sinica **66**, 413 (2008).
[125] Y. R. Mo and J. L. Gao, J. Phys. Chem. A **105**, 6530 (2001).
[126] Y. Zhang and X.-Y. You, J. Comput. Chem. **22**, 327 (2001).
[127] E. D. J. Sloan, *Clathrate Hydrates of Natural Gases*, 2nd ed. (Marcel Dekker, New York, 1998).
[128] E. D. J. Sloan, Energy Fuels **12**, 191 (1998).
[129] E. D. J. Sloan, Ind. Eng. Chem. Res. **39**, 3123 (2000).
[130] J. P. Kennett, K. G. Cannariato, I. L. Hendy, and R. J. Behl, *Methane Hydrates in Quaternary Climate Change: The Clathrate Gun Hypothesis* (American Geophysical Union, Washington, DC, 2003).
[131] G. C. Pimentel and S. W. Charles, Pure Appl. Chem. **7**, 111 (1963).
[132] I. U. Goldschleger, G. Kerenskaya, V. Senekerimyan, K. C. Janda, and V. A. Apkarian, Phys. Chem. Chem. Phys. **10**, 7226 (2008).
[133] K. C. Janda, G. Kerenskaya, I. U. Goldschleger, V. A. Apkarian and E. Fleischer, in *Proceedings of the 6th International Conference on Gas Hydrates* (ICGH 2008), Vancouver, British Columbia, Canada, 2008 (https://circle.ubc.ca/bitstream/2429/1476/1/5393.pdf).
[134] V. Senekerimyan, I. Goldschleger, and V. A. Apkarian, J. Chem. Phys. **127**, 214511 (2007).
[135] D. P. Cherney, S. E. Duirk, J. C. Tarr, and T. W. Collete, Appl. Spectrosc. **60**, 764 (2006).
[136] A. Valdes, R. Prosmiti, P. Villarreal, G. Delgado-Barrio, and H.-J. Werner, J. Chem. Phys. **126**, 204301 (2007).
[137] A. K. Pathak, T. Mukherjee, and D. K. Maity, J. Phys. Chem. A **112**, 744 (2008).
[138] S. Simon, J. Bertran, and M. Sodupe, J. Phys. Chem. A **105**, 4539 (2001).
[139] R. Franklin-Mergarejo, J. Rubayo-Soneira, N. Halberstadt, T. Ayed, M. I. Bernal-Uruchurtu, R. Hernández-Lamoneda, and K. C. Janda, J. Phys. Chem. A (in press) 2009.
[140] M. I. Bernal-Uruchurtu and I. Ortega-Blake, J. Phys. Chem. A **103**, 884 (1999).

[141] D. Chandler, Nature **437**, 640 (2005).
[142] D. P. Schofield and K. D. Jordan, J. Phys. Chem. A **111**, 7690 (2007).
[143] T. Renger, B. Grundkötter, M. E.-A. Madjet, and F. Müh, Proc. Nat. Acad. Sci. **105**, 13235 (2008).
[144] C. J. Cramer and D. G. Truhlar, Acc. Chem. Res. **41**, 760 (2008).
[145] A. Klamt, B. Mennucci, J. Tomasi, V. Barone, C. Curutchet, M. Orozco, and F. J. Luque, Acc. Chem. Res. **2009**, DOI: 10.1021/ar800187p.
[146] A. J. Huneycutt and R. J. Saykally, Science **299**, 1329 (2003).
[147] D. P. Schofield, and K. D. Jordan, J. Phys. Chem. A (accepted) 2009, DOI: 10.1021/jp900237j.